

Angostura Dam to Montaña Bridge: Geomorphic and Hydraulic Analysis

**Upper Colorado Region
Albuquerque Area Office
Technical Services Division
Middle Rio Grande Project, NM**



Mission Statements

The mission of the Department of the Interior is to protect and manage the Nation's natural resources and cultural heritage; provide scientific and other information about those resources; and honor its trust responsibilities or special commitments to American Indians, Alaska Natives, and affiliated island communities.

The mission of the Bureau of Reclamation is to manage, develop, and protect water and related resources in an environmentally and economically sound manner in the interest of the American public.

Angostura Dam to Montaño Bridge: Geomorphic and Hydraulic Analysis

Middle Rio Grande Project, NM
Technical Services Division
Albuquerque Area Office
Upper Colorado Region

Report Prepared by:

Aubrey Harris, PE, Hydraulic Engineer
Michelle Klein, PE, Hydraulic Engineer
Chi Bui, PE, Sr. Hydraulic Engineer

Report Reviewed by:

Robert Padilla, PE, DWRE, Supervisory Civil (Hydraulic) Engineer
Ari Posner, PhD, Physical Scientist
Mark Nemeth, PE, PhD, Technical Services Division Manager

Cover Picture: Taken by Chi Bui in July 2017. At RM 199 (BB-342) east bank, looking downstream on the Rio Grande, located on Sandia Pueblo.

Contents

0.0 Executive Summary	7
0.1 Content Guide	9
1.0 Background	11
2.0 Hydraulic Analysis.....	15
2.1 Channel Geometry and Hydraulic Parameters.....	15
3.0 Geomorphic Analysis.....	18
3.1 Longitudinal Profile	18
3.2 Slope	22
3.3 Channel Width	25
3.4 Sinuosity	29
3.5 River Planform.....	30
3.6 Sediment Supply and Transport.....	46
4.0 Hydrologic Analysis	60
4.1 Floodplain Terraces	61
5.0 Future Channel Response	66
6.0 Acknowledgements.....	68
7.0 References.....	68

Tables

Table 1 Reach-averaged results from hydraulic parameters from 1-D HEC-RAS modeling at different discharges for 2004, 2009, 2012 (Tetra Tech, 2013) 2015, and 2017.	17
Table 2 Historical mean thalweg slopes modified from Tetra Tech (2013).	22
Table 3 Features in Subreach 0, relative to CO-lines.	23
Table 4 Reach averaged thalweg slope results from hydrographic data collection for the thalweg profile and the water surface elevation for Subreaches 1, 2, and 3, as presented in Figure 6.	24
Table 5 Average Channel Width Values for the HWY 550 to Montañ0 reach	25
Table 6 Sinuosity of the reach from Highway 550 to Montañ0 Bridge (modified from Tetra Tech 2013; Reclamation 2017).....	29
Table 7 Results of averaged meander bend geometry observations for the study reach.	33
Table 8 Definition of Massong Planform Stages and additional Evaluation Criteria used in the analysis (Massong et al., 2010).....	41
Table 9 Digitized active channel area in comparison to vegetated islands and bars, modified from Tetra Tech (2013).	46
Table 10 Summary of changes in bed material size for varying subreaches of the Rio Grande. .	47
Table 11 Average suspended sediment concentration of the Rio Grande at Albuquerque gage (USGS 08330000). Modified from Makar and AuBuchon 2012.	49
Table 12 Sample results for Bed Material Sizes during 2016 Spring Runoff (modified from Occam 2016).....	52

Table 13 Computed Total Loads at the Incoming and Outgoing Cross Sections of the Reach between Highway 550 Bridge and Montaña Bridge.....	56
---	----

Figures

Figure 1 Map of study reach "subreaches" and location identifiers.	14
Figure 2 Reach-averaged results for hydraulic parameters from 1-D HEC-RAS modeling at different discharges for 2004, 2009, 2012 (Tetra Tech, 2013) 2015, and 2017.	16
Figure 3 Longitudinal profile of the Rio Grande within the reach.	21
Figure 4 Slope analysis of Cochiti (CO) rangelines in Subreach 0.	22
Figure 5 Longitudinal profile for Subreach 0 thalweg in notable years.	23
Figure 6 Reach distance weighted, averaged thalweg slope results from hydrographic data collection for a) the thalweg profile; and b) the water surface elevation.....	24
Figure 7 Average Active Channel Width from Highway 550 to Montaña Bridge.....	26
Figure 8 (a) Total perpendicular distance between levees and (b) Distance to right and left levees from the 2012 Rio Grande centerline.....	28
Figure 9 Sinuosity for the study reach; values presented in Table 5.	29
Figure 10 Planform outlines for the reach in various years. River narrowing and reduction of large in-stream features such as islands and attached sandbars is evident for the entire reach from Angostura to Montaña Bridge.	31
Figure 11 Meander belt widths based on location in the reach; negative values indicate bends on river left. Areas of divergence (1-8) are discussed in following figures.	35
Figure 12 Bend changes near CO-25 to opposite active channel bank; bend formation shown near TA-253 in 2016. This is below Jemez Canyon. (1)	36
Figure 13 Near TA-275. Bend migrating downstream, resulting in a tighter meander, as the river's left bend at TA-277.5 is fixed, this location coincides with Santa Ana Projects. Yellow arrow is approximately at the same position in all images. (2)	37
Figure 14 Near BB-316, where the braided planform shifted to a straight channel by 2006, and then Reclamation construction activities in 2008 constructed bends with bendway weir structures at Sandia Priority Site, with an inception of non-constructed bends at BB-313 and BB-318 as well. (3).....	37
Figure 15 Planform change near CR-372, from braided and dynamic planforms in 1992 and 2006 to the singular channel in 2016. (6)	38
Figure 16 Changes in the planform above Alameda Bridge, where the braided planform has become established by vegetation, and connected side channels in 2016 imagery. (8).	39
Figure 17 2016 Belt width analysis combined with levee distance analysis. Area in commentary highlighted in yellow.	40
Figure 18 Middle Rio Grande planform cycle model (from Massong et al., 2010).	41
Figure 19 Planform classifications for the Angostura Dam to Montaña Reach.	42
Figure 20 River planform analysis for the Angostura Dam to Montaña Reach, 1992 to 2016. ...	43
Figure 21 National Wetlands Inventory Program maps produced by Army Corps of Engineers for Berry and Lewis (1997).	45
Figure 22 Active channel area in comparison to vegetated islands and bars, modified from Tetra Tech (2013).	46
Figure 23 Recent bed material collection by grain size, year, and location.	48

Figure 24 Percent bed material grain sizes for samples collected in February and March 2016 (modified from Tetra Tech, 2016).	49
Figure 25 Annual totals for suspended sediment loads and the water discharge from the USGS gage at Albuquerque (USGS 08330000) from 1970 to 2013.	50
Figure 26 Monthly average box and whisker plots from 1970 to 2014 for the Albuquerque USGS gage. Whiskers indicate maximum and minimum, centerline in the box indicates median and surrounding quartiles representing the 25% and 75% values.	50
Figure 27 Effective discharge calculations demonstrating the hydrologic seasons and the sediment transported per unit discharge.	51
Figure 28 Box and whisker (error bars showing maximum and minimum values; Q1 (25%), median and Q3 (75%) represented by box bounds) averaging the results from sample collection during 2016 Spring Runoff (modified from Occam 2016).	52
Figure 29 Computed Total Loads at the Incoming and Outgoing Cross Sections of the Reach between Highway 550 Bridge and Montaño Bridge.....	55
Figure 30 Channel Bed Elevation of the Study Reach in recent years	58
Figure 31 Number of days each year exceeding set discharges for the USGS gage on the Rio Grande at Albuquerque for period of record (USGS 08330000).	60
Figure 32 Percent exceedance for particular discharge intervals from 1993 to 2013. Modified from Bui 2014.	61
Figure 33 Terrace analysis results for the study reach. Figures A-E progress downstream through the reach.	66

0.0 Executive Summary

The Angostura Dam to Montaño Bridge reach (Reach) is located in a section of river that has mixed land use, involving both agricultural and urbanized activities. Various federal, state, and local agencies as well as two Native American tribes (Pueblos) have established water resource infrastructure including levees, canals, and drains, surface water diversion dams, subsurface pipelines, stormwater outfalls, and effluent discharge points. These same agencies have performed numerous habitat restoration, fire reduction, and recreational projects in this reach both in the active river channel and in the floodplain. The purpose of this report is to identify past, current, and potential future geomorphic and hydraulic trends and conditions in the Reach to support the U.S. Bureau of Reclamation (Reclamation) as it performs its authorized mission under the Middle Rio Grande Project. Understanding these trends and conditions will inform future planning for river maintenance and habitat restoration work in this reach.

The geomorphic planform trends characterized in this report generally conform to Schumm's (1977) model and Massong et al. (2010) progressing planform model in hypothesizing changes due to decreasing peak water discharges and sediment discharges. Since the construction of Cochiti Dam, the reach has changed from a braided (multi-thread) mobile sand bed channel to a sinuous single thread channel that is narrowing and incising (deepening). This planform change is consistent with the river undergoing a geomorphic threshold transition to a meandering (bend and point bar) type pattern with incisional tendencies. The channel has become disconnected from the historic floodplain, while woody vegetation has encroached along the banklines, further narrowing the channel and stabilizing sand bars.

Generally, these geomorphic trends and conditions are continuing downstream of the Arroyo de la Barranca near the Corrales Siphon with bed incision and coarsening, and the development of new bends and their subsequent lateral migration. These trends and conditions may eventually pose a problem for the adjacent river side levees, canals, and drains that laterally constrain this river corridor. Impacts to water delivery and associated works outside the levee system in this semi-urbanized reach of the Rio Grande are of concern to Reclamation. Given these long-term morphologic changes in this reach, both aquatic and riparian habitat areas are experiencing effects related to their function and connectivity with the active river channel and flows. In the last few decades multiple agencies (including Reclamation) and the Native American Pueblos have done extensive mechanical habitat restoration projects in the reach that include the creation of embayments, side channels, bar and island destabilization, jetty jack removal and vegetation plantings. These efforts are intended to emulate natural historical river processing that created both aquatic and riparian habitats.

The following provides a summary of the significant hydraulic and geomorphic findings determined by the analyses in this report.

- Between 2004 and 2017, the reach-average river hydraulic parameters have the following trends (for all discharges modeled): the channel top width decreased, the hydraulic depth increased, the width to depth ratio decreased, the energy grade slope

increased, the wetted perimeter decreased, the flow area decreased, and the channel velocity increased (2.1 Channel Geometry and Hydraulic Parameters, p. 15).

- The minimum channel bed elevation (thalweg elevation) lowered between the Angostura Diversion Dam and the Albuquerque Metropolitan Arroyo Flood Control Authority (AMAFCA) North Diversion Channel from 1971 to 2017. Immediately downstream of the AMAFCA North Diversion Channel, the thalweg elevation is approximately the same elevation in 2017 as it was in 1971. (3.1 Longitudinal Profile, p. 18).
- The average slope has remained relatively consistent throughout the reach from 2004 to 2017 (3.2 Slope, p. 22).
- The average active channel width decreased over time from 1,338 ft in 1918 to 267 feet in 2018 (3.3 Channel Width, p. 25).
- An analysis of distances from the channel centerline to the nearest levee or other infrastructure identified areas which may warrant monitoring for future river maintenance needs. In the reach between U.S. Highway 550 (HWY 550) and Montaña Bridge, there are many private residences in close proximity to the levee systems and river.

Noteworthy areas with small distances between the channel centerline to the nearest infrastructure include the left (to the east) levee at the Bernalillo Priority Site, the left levee at the Sandia Priority Site, the right (to the west) levee at the Corrales Siphon crossing, the right levee at RM 199 (BB-346), the right levee at RM 195 across from the Sandia Fishing Ponds, the right levee upstream of the Alameda footbridge at RM 192, the Albuquerque-Bernalillo County Water Utility Authority (ABCWUA) Diversion Dam intake, and the left levee around RM 189 (3.3.1 Levee Width Analysis, p. 26).

- The river is most sinuous in the upstream portions starting at Angostura and generally decreases in sinuosity in the downstream direction. Between 1972 and 2016, the reach's average sinuosity increased (3.4 Sinuosity, p. 29).
- In 1918 the river planform was a wide braided channel. In 2017, due to anthropogenic and natural factors, the reach has planforms ranging from narrow meandering single thread channel between HWY 550 and the AMAFCA North Diversion Channel, transitioning to a wider channel with vegetated islands between the AMAFCA North Diversion Channel and Montaña (3.5 River Planform, p. 30).
- Bed material in the reach has coarsened over time. The median bed material size in the reach is largest at the upstream end of the reach and decreases in the downstream direction (3.6.1 Bed material, p. 46).
- The average suspended sediment concentration in the reach decreased by one order of magnitude after the closure of Cochiti Dam in the 1970s. The post-runoff season (July through October) is the most effective at transporting sediment (3.6.2 Suspended sediment, p. 49).
- From 2002 to 2012, the river channel from Angostura Diversion Dam to about the Harvey Jones Channel experienced a net volume loss of sediment. From about the Harvey Jones Channel to Isleta Diversion Dam, the channel experienced a net volume gain. Varyu (2018) predicts the same trends for the next twenty years (2012 to 2032) but with the transition point at the ABCWUA Diversion Dam instead of the Harvey Jones Channel. The potential implications of this predictive modeling could

include bed and bank erosion and loss of floodplain connectivity upstream of ABCWUA diversion dam, with reduced channel capacity and increased floodplain connectivity downstream of ABCWUA diversion dam (3.6.4 SRH-1D Technical Report Summary, p. 59).

- As upstream surface water dams and diversions increased on the Upper Rio Grande and Rio Chama systems, the variability of discharges on the Middle Rio Grande and in this reach has decreased, meaning that the river is wet for a greater period of the year but at lower peak discharges than previously observed (4.0 Hydrologic Analysis, p. 59).
- Generally it was found that the areas between the levees and the river are higher in elevation than the channel (the channel is not perched). The upstream end of the reach has the highest terraces above a given water surface elevation (WSE) and the terrace heights above a given WSE generally decrease in the downstream direction (4.1 Floodplain Terraces, p. 61).
- The expected future channel trends include bed incision, bed material coarsening, increasing in-stream velocities and depths, and increased meandering. Future problems arising from these expected trends include riverside infrastructure being threatened and floodplain disconnection due to incision (5.0 Future Channel Response, p. 66).

0.1 Content Guide

The following table identifies cross section locations and salient reach features that are mentioned in report sections. This table can be used to easily look up noticeable trends and conditions based on river location and feature. Section 5.0 of this report summarizes the general geomorphic and hydraulic trends and conditions, potential river maintenance needs and habitat restoration opportunities, and some example river engineering and maintenance methods to consider in future planning for the reach.

LOCATION (Reclamation Cross Section Rangeline)	FEATURES	SECTION MENTIONED
CO-24 to BB-300	Subreach 0: Angostura Diversion Dam to HWY 550	Background (1.0) Longitudinal Profile (3.1) Slope Analysis (3.2.1) Sinuosity (3.4) River Planform (3.5) Floodplain Terraces (4.1)
CO-25	Below Jemez Canyon	Meander Bends (3.5.1)
TA-275	Santa Ana Projects	Slope Analysis (3.2.1) Meander Bends (3.5.1) Bed Material (3.6.1)
BB-300 to BB-327	Subreach 1: HWY 550 to above Arroyo de la Barranca (Subreach Locations based on Tetra Tech 2013)	Background (1.0) Hydraulic Analysis (2.0) Longitudinal Profile (3.1) Slope Analysis (3.2.2) Channel Width (3.3) Sinuosity (3.4)

LOCATION (Reclamation Cross Section Rangeline)	FEATURES	SECTION MENTIONED
		River Planform (3.5) Meander Bends (3.5.1) Floodplain Terraces (4.1)
BB-303	Bernalillo Priority Site	Background (1.0) Meander Bends (3.5.1)
BB-304 to BB-305		Slope Analysis (3.2.2)
BB-306	Bosque Encantado	Levee Width Analysis (3.3.1) River Planform (5.1)
BB-307 to BB-317	Sandia Priority Site, also Arroyo Venada	Background (1.0) Longitudinal Profile (3.1) Levee Width Analysis (3.3.1) River Planform (3.5) Meander Bends (3.5.1)
BB-327 to CR-372	Subreach 2 (Subreach Locations based on Tetra Tech 2013)	Background (1.0) Hydraulic Analysis (2.0) Longitudinal Profile (3.1) Slope Analysis (3.2.2) Channel Width (3.3) Sinuosity (3.4) River Planform (3.5) Habitat Restoration (5.4.2)
BB-327 to BB-345 includes CO-32	Area surrounding Arroyo de la Barranca RM 199 is near BB-345	Longitudinal Profile (3.1) Meander Bends (3.5.1) Bed Material (3.6.1)
CO-33	Sandia Pueblo	Meander Bends (3.5.1)
BB-338 to CR-355	Arroyo de la Barranca to Harvey Jones	Longitudinal Profile (3.1) River Planform (3.5) Meander Bends (3.5.1)
BB-340	Corrales Siphon	Background (1.0) Levee Width Analysis (3.3.1) Bed Material (3.6.1) Floodplain Terraces (4.1)
CR-355	Harvey Jones Channel/Arroyo de los Montoyas	Longitudinal Profile (3.1) Meander Bends (3.5.1) Habitat Restoration (5.4.3) Total load Calculations (3.6.3)
CR-367 to CR-400	AMAFCA North Diversion Channel	Background (1.0) Longitudinal Profile (3.1) Levee Width Analysis (3.3.1) Meander Bends (3.5.1) Floodplain Terraces (4.1) Habitat Restoration (5.4.3)
CR-372 to AQ-427	Subreach 3 (Subreach Locations based on Tetra Tech 2013)	Background (1.0) Hydraulic Analysis (2.0) Longitudinal Profile (3.1) Slope Analysis (3.2.2) Channel Width (3.3) Sinuosity (3.4)

LOCATION (Reclamation Cross Section Rangeline)	FEATURES	SECTION MENTIONED
CO-34 to CA-9	Area Surrounding Alameda Bridge	Bed Material (3.6.1) Meander Bends (3.5.1) Floodplain Terraces (4.1) Habitat Restoration (5.4.2)
CA-1 to CA-2;	Alameda Bridge also USGS 08329918	Bed Material (3.6.1) Total Load Analysis (3.6.3)
CA-6	Calabacillas Arroyo	Longitudinal Profile (3.1) Slope Analysis (3.2.2) River Planform (3.5)
CA-11 to CA-12	Montaño Bridge	River Planform (3.5) Bed Material (3.6.1)
AQ-472.4		Total Load Analysis (3.6.3)
CO-36 (beyond scope of this reach)	Albuquerque Gage USGS 08330000	Suspended Sediment (3.6.2) Hydrologic Analysis (4.0)

1.0 Background

The Middle Rio Grande Valley experienced significant population and land use change over the last century, starting with the historic Pueblos of Santa Ana and Sandia and continuing through the establishment of the towns of Corrales, Rio Rancho, Albuquerque, and Bernalillo. In this valley since the 1930s, land development has shifted from agricultural to urbanized uses. Water resource development in the forms of flood protection, channelization, irrigation and drainage, municipal water supply and discharge activities have progressed with these land use changes in this reach.

Dramatic, channel-forming, and unregulated flood events occurred in the Middle Rio Grande Valley in early history, with recorded events in the 1880s and early 1900s exceeding 10,000 cfs and occurring at about a 2-year frequency (Berry and Lewis, 1997). These high discharge events decimated crops and communities. In the 1930s, the Middle Rio Grande Conservancy District (MRGCD) excavated riverside drains and constructed non-engineered levees from the spoil materials in the Rio Grande valley as part of their district-wide plan to drain valley farmlands and to provide some form of flood protection. Farmlands required draining due to high groundwater levels which causes high alkalinity in the soil. The high groundwater levels were the result of channel aggradation. The levee and drain construction supplemented existing levees or *burros*, and canals that existed in the Rio Grande Valley before district-wide construction (Berry and Lewis, 1997).

Along the study reach from the Angostura Diversion Dam to Montaño Bridge, riverside drains and levees are present in most of the reach starting from Santa Ana Pueblo to Montaño Bridge, with an exception being the right side of the river floodplain from Angostura Dam to Corrales Siphon. The levees protect the City of Albuquerque, the Town of Bernalillo, the Village of Corrales, and the Pueblos of Sandia and Santa Ana. These features confine the river and limit future opportunities for expanding the width of the floodplain. Channel migration and bank erosion are problematic on both sides as they

present a risk for the levee, drain, and canal infrastructure. Further discussion of levee features can be found in Section 3.3.1.

The Angostura Diversion Dam to Montañito Bridge river reach is in a predominantly urban corridor. Many sources of water and sediment to the reach have infrastructure controls upstream. In 1934, irrigation diversion dams were built at Cochiti Pueblo and Angostura. The Jemez Canyon Dam was built in the 1950s to provide flood and sediment control on the Jemez River, which drains into the Rio Grande downstream of Angostura (Makar and AuBuchon, 2012). Cochiti Dam, which began impounding water in 1973, provides flood and sediment control on the main stem of the Rio Grande. In 2001, Jemez Canyon Dam changed its operations, by draining its sediment pool and beginning operation as a dry dam, this increased sediment load to the Rio Grande relative to the period following Jemez Canyon Dam construction.

The Reach includes the AMAFCA North Diversion Channel, which drains rainfall runoff from most of northeast Albuquerque and is predominately a concrete-lined channel. Also included is the Albuquerque-Bernalillo County Water Utility Authority's adjustable-height diversion dam and pump station, which diverts Rio Grande surface water to the San Juan-Chama Drinking Water Treatment Plant.

The Reach has experienced geomorphic changes such as the degradation of the bed elevation, decrease in channel width, and increase in bed material size (Tetra Tech, 2013). River maintenance activities have been performed to protect the integrity of riverside and water delivery infrastructure along the river due to rapid bank erosion and migrating bends. In 2007, thirteen bendway weirs were installed at the Bernalillo Priority Site to protect the eastern levee system around BB-303/RM 203 (Sixta and Nemeth, 2005). In 2008, fifty bendway weirs were installed at the Sandia Priority Site to protect the eastern levee system from approximately BB-307 to BB-317 (near RM 203 to RM 202) (Nemeth and Sixta, 2005). For both the Bernalillo and Sandia sites there were habitat restoration components which included secondary channels, backwater embayments, and vegetation plantings. In 2016, a pre-emergency construction occurred at MRGCD's Corrales Siphon (near BB-339 at RM 200) to protect the exposed siphon from potential damage due to the upcoming 2016 spring runoff. Long term trends of river bed degradation in the Reach exposed the subsurface siphon pipeline (MRGCD, 2014). Erosion occurring at BB-346 (RM 199) on the west bankline was identified as a river maintenance site due to active erosion occurring in a bend-like formation during the 2016–2017 spring runoff seasons and its proximity to the Corrales levee system.

This geomorphic and hydraulic document represents Reclamation's update to the 2013 work performed by Tetra Tech for the HWY 550 to Montañito Bridge reach geomorphic assessment. Reclamation's update uses data collected between 2013 and 2017. Also, Reclamation expanded the study reach upstream to include the reach between Angostura Dam and HWY 550 (the Pueblo of Santa Ana).

Tetra Tech's 2013 report used data collected between 2004 and 2012, and it divided the study area into three subreaches based on dominant bed material type and channel morphology. Those

subreaches were designated as Subreach 1, Subreach 2, and Subreach 3. When the Rio Grande reach from Angostura Dam to Highway 550 was added to the study, this upstream reach was designated as Subreach 0.

Subreach 0: Reach from Angostura Dam to HWY 550, data supplied from Santa Ana Pueblo. CO-24 to BB-300. Subreach 0 was not included in the original 2013 Tetra Tech report. May be characterized as an incised single thread channel, gravel dominated.

Subreach 1: Reach from HWY 550 at BB-301 (RM 203.5) to above Arroyo de la Barranca, BB-327 (RM 200.9). Located between the communities of Rio Rancho and Corrales. Subreach 1 was characterized as single-thread gravel-cobble dominated (Tetra Tech 2013).

Subreach 2: Reach from above Arroyo de la Barranca at BB-327 to approximately AMAFCA North Diversion Channel, CR-372 (RM 196.6). Subreach 2 was characterized as having both single-thread and braided planform; the dominant bed material size has changed from sand-dominated to gravel-dominated (Tetra Tech 2013).

Subreach 3: Reach from around AMAFCA North Diversion Channel at CR-372 to Montaña Bridge (RM 187.9), approximately AQ-427. Subreach 3 was characterized as a multi-thread, sand-dominated system (Tetra Tech 2013).

Information from the early 1900s, such as aerial photography, has been incorporated as well in this document. The analysis work includes the performance of hydraulic modeling and geomorphic assessment. The objective is to identify key hydraulic and geomorphic factors that lead to the observed geomorphic changes in the reach, as well as the anticipated future channel response from the current condition, with the objective to aid in the identification of river maintenance sites and potential locations for habitat restoration.

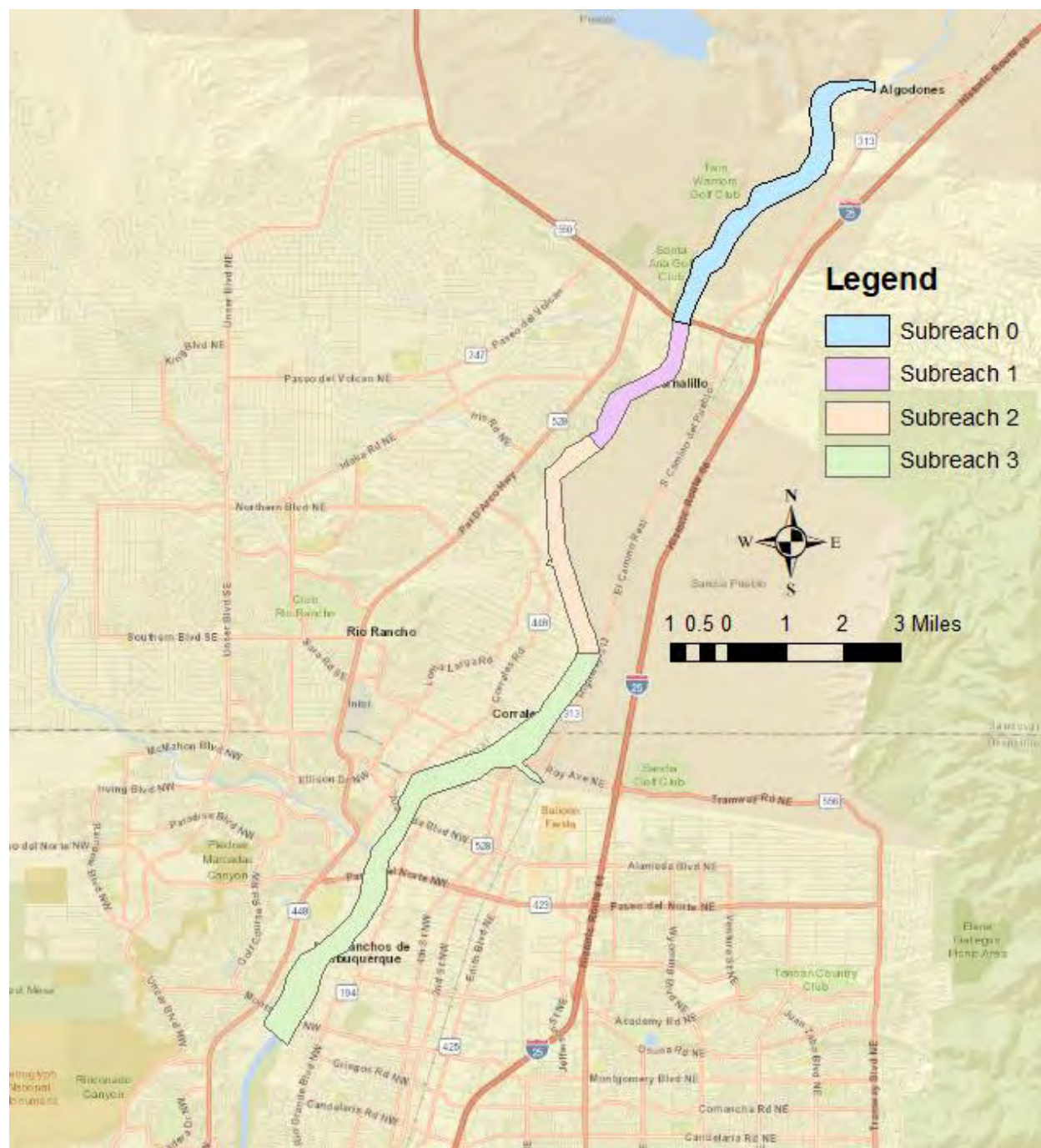


Figure 1 Map of study reach "subreaches" and location identifiers.

2.0 Hydraulic Analysis

Hydraulic analysis involves theoretical and quantitative analysis of the mechanical properties of open channel flow. This analysis examines the change in hydraulic properties of the river over time including top width, hydraulic depth, width-depth ratio, slope, wetted perimeter, flow area, and channel velocity. These hydraulic properties are affected by many factors including, but not limited to, the hydrologic regime, the grain size of the bed material, the surrounding geology, the valley's slope, the bank stability due to vegetation, and the roughness of the fluvial boundary due to vegetation. The channel's hydraulic properties can be used to determine the reach's capacity for water and sediment transport. Knowledge of these results can aid in the design of stable channels and suitable habitat.

2.1 Channel Geometry and Hydraulic Parameters

Tetra Tech (2013) ran HEC-RAS 1-dimensional (1-D) models for the years 2004, 2009, and 2012, and compiled the results. The work conducted in this report updates the figures with data collected in 2015 and 2017. Hydrographic data was collected by Reclamation contractors on rangelines throughout the reach and was used to build two HEC-RAS 1-dimensional models representing the 2015 and 2017 geometries.

The models were calibrated to match the water surface elevation of the field collected data set iteratively by adjusting Manning's n value. The information was compiled into Figure 2 and Table 1 to identify trends of changing channel capacity and other variables that describe the reach. Reach-averaged values are presented.

Only cross-sections with consistent data present for all 5 models (2004–2017) were evaluated for reach-wide averages. The hydraulic parameters were averaged based on channel distances between each cross-section. The upstream boundary was the HWY 550 Bridge at rangeline BB-301. The downstream boundary is Montañño Bridge at CR-462. The discharges modeled reflect a median discharge (1,000 cfs) at Rio Grande at Alameda Bridge (USGS 08329918), the channel-forming discharge corresponding to the 2-year event (3,700 cfs), and a 100-year flood event discharge (10,000 cfs presented in the Figures) (Wright et al. 2010). Flood-frequency for the 2-year event and 100-year event were evaluated by Pearson Type III analysis (Belmont, 2005), using the Rio Grande at Albuquerque (USGS 08330000) and Rio Grande San Felipe (USGS 08319000) gages. The arithmetic average of the 2-year events for both Albuquerque and San Felipe was utilized; the resulting average was rounded to the nearest hundred cubic foot per second. The period of evaluation was from 1988 to 2017. It should be noted for calibrating the hydraulic model, that there is one stream gage at Rio Grande at Alameda Bridge (USGS 08329918) in the study reach for which discharges were used in the calibration process. Discharge measurements were not available at each cross section for ideal calibration.

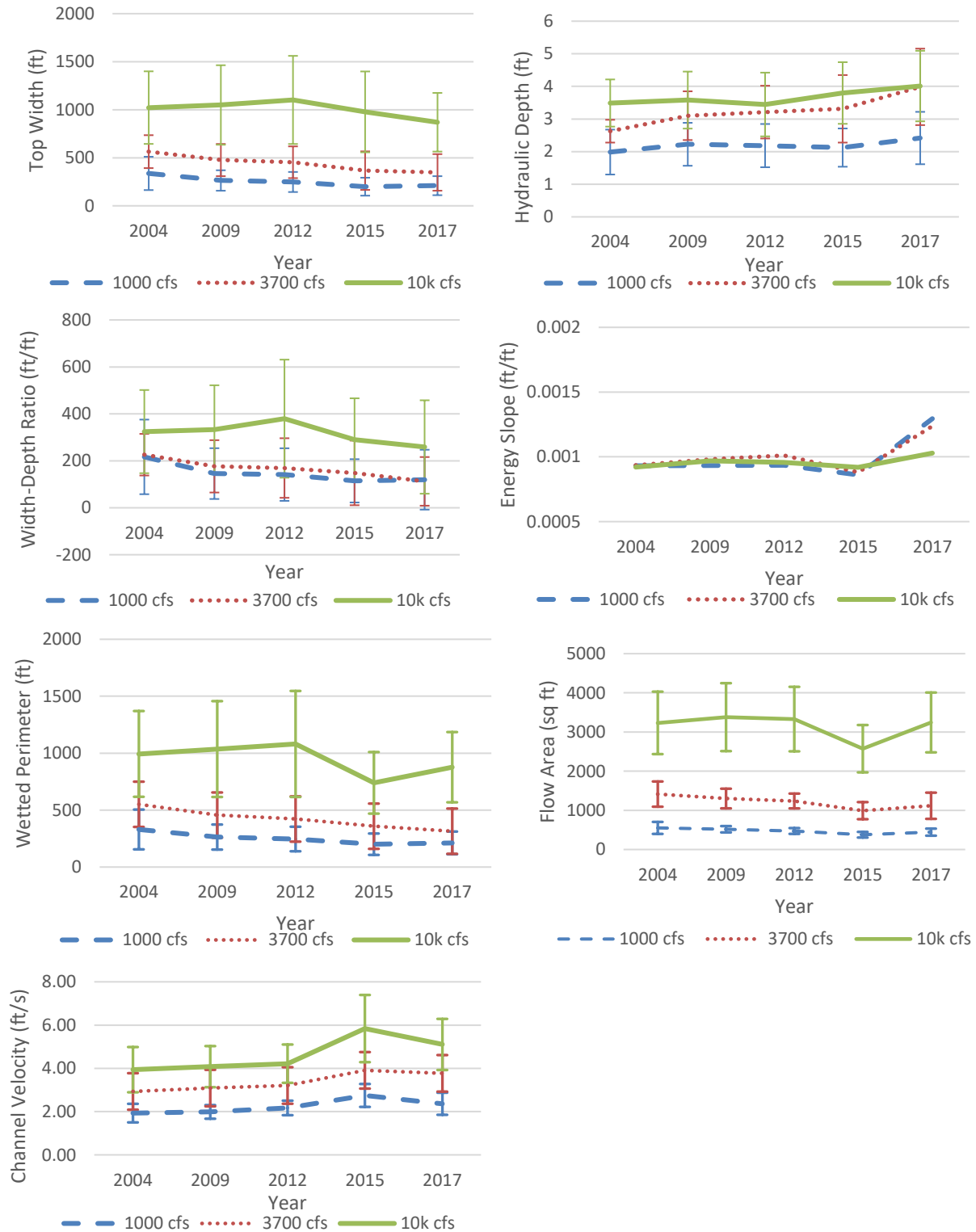


Figure 2 Reach-averaged results for hydraulic parameters from 1-D HEC-RAS modeling at different discharges for 2004, 2009, 2012 (Tetra Tech, 2013) 2015, and 2017.

Table 1 Reach-averaged results from hydraulic parameters from 1-D HEC-RAS modeling at different discharges for 2004, 2009, 2012 (Tetra Tech, 2013) 2015, and 2017.

1,000 cfs	Top Width (ft)	Hydraulic Depth (ft)	W/D (ft/ft)	Energy Slope (ft/ft)	Wetted Perimeter (ft)	Flow Area (ft ²)	Velocity (ft/s)
2004	350	1.7	240	0.00095	340	560	1.9
2009	240	2.2	130	0.00087	240	510	2.0
2012	240	2.1	140	0.00088	230	480	2.2
2015	190	2.1	110	0.00083	190	380	2.7
2017	200	2.4	110	0.0010	200	450	2.3
3,700 cfs	Top Width (ft)	Hydraulic Depth (ft)	W/D (ft/ft)	Energy Slope (ft/ft)	Wetted Perimeter (ft)	Flow Area (ft ²)	Velocity (ft/s)
2004	560	2.6	230	0.00094	550	1,400	2.9
2009	480	3.1	180	0.00098	460	1,300	3.1
2012	450	3.2	170	0.0010	420	1,200	3.2
2015	370	3.3	150	0.00088	360	990	3.9
2017	350	4.0	110	0.0012	320	1,100	3.8
10,000 cfs	Top Width (ft)	Hydraulic Depth (ft)	W/D (ft/ft)	Energy Slope (ft/ft)	Wetted Perimeter (ft)	Flow Area (ft ²)	Velocity (ft/s)
2004	980	3.4	320	0.00034	960	3,300	4.0
2009	1,100	3.3	360	0.00032	1,100	3,600	4.0
2012	1,200	3.1	430	0.00030	1,200	3,600	4.1
2015	1,000	3.5	330	0.00034	740	2,600	5.7
2017	880	3.8	280	0.00076	890	3,300	5.0

Pre-2012, for flows of 1,000 and 3,700 cfs, the top width (W) of the river decreased while hydraulic depth (D) increased, which is consistent with bed incision and narrowing. Velocities experienced an increasing trend as flows are concentrated efficiently in the narrow channel. Generally, the slope (S) in the reach was decreasing from 2004 to 2015. According to Schumm (1977), this is correlated with a decreased sediment load (Qs) in the reach. Schumm further predicts that a decrease in sediment load will decrease meander wavelength and increase the sinuosity of the river.

If Qs ↓, then: W ↓; D↑; and S ↓

It appears that generally, trends of hydraulic parameters shifted in between 2012 to 2015. After 2012, the top width at 1,000 expanded again, but not to previous widths; for higher flows, the top width continued to be narrower than those prior to 2012, indicating that flows at 10,000 cfs are not inundating as much as in 2004. The top width at the 2-yr flow of 3,700 cfs decreased by approximately 100 feet between 2012 to 2015. Hydraulic depth and velocities continued to increase. The trends for the most recent years do not fit Schumm's predictions as well as what was found in the pre-2012 trends. To reach a conclusion here, it was necessary to incorporate trends for both sediment and water discharge (discussion in Sections 3.6 and 5.0 respectively).

If Q↓ and Qs↓, then: W ↓; λ↓; P↑; W/D↓

where λ is the meander wavelength, P is the sinuosity, and W/D is the width to depth ratio.

Further discussion of trends in meander wavelength (Section 3.5.1), sinuosity (Section 3.4), and channel width (Section 3.3) are discussed later in the report. Observations agree with Schumm's model.

3.0 Geomorphic Analysis

Geomorphology is the study of terrain evolution due to processes occurring near the Earth's surface. Changing fluvial landforms can be described by physical trends of sediment transport (whether erosion, conveyance, or deposition) as affected by the movement of water in the river's system. Geomorphic analysis includes evaluating sediment transport, discharge characteristics, and particle size data and trends; river planform and cross section data and their changes over time; determining ongoing physical processes and their relation to man-made features; and channel adjustment/response to changing flow and sediment regimes. All of these can inform possible causes for currently occurring river processes and trends and may also forecast future river needs that are developing in this reach.

3.1 Longitudinal Profile

The longitudinal thalweg profile shows reach-wide trends of river bed elevation, as well as possible effects of in-stream structures and contributing tributaries. It may aid in defining the drivers and controls for local bed changes that appear to be random. The longitudinal thalweg profile of the Rio Grande in the study reach was evaluated based on hydrographic cross-sectional data collected from 2004 to 2017 (

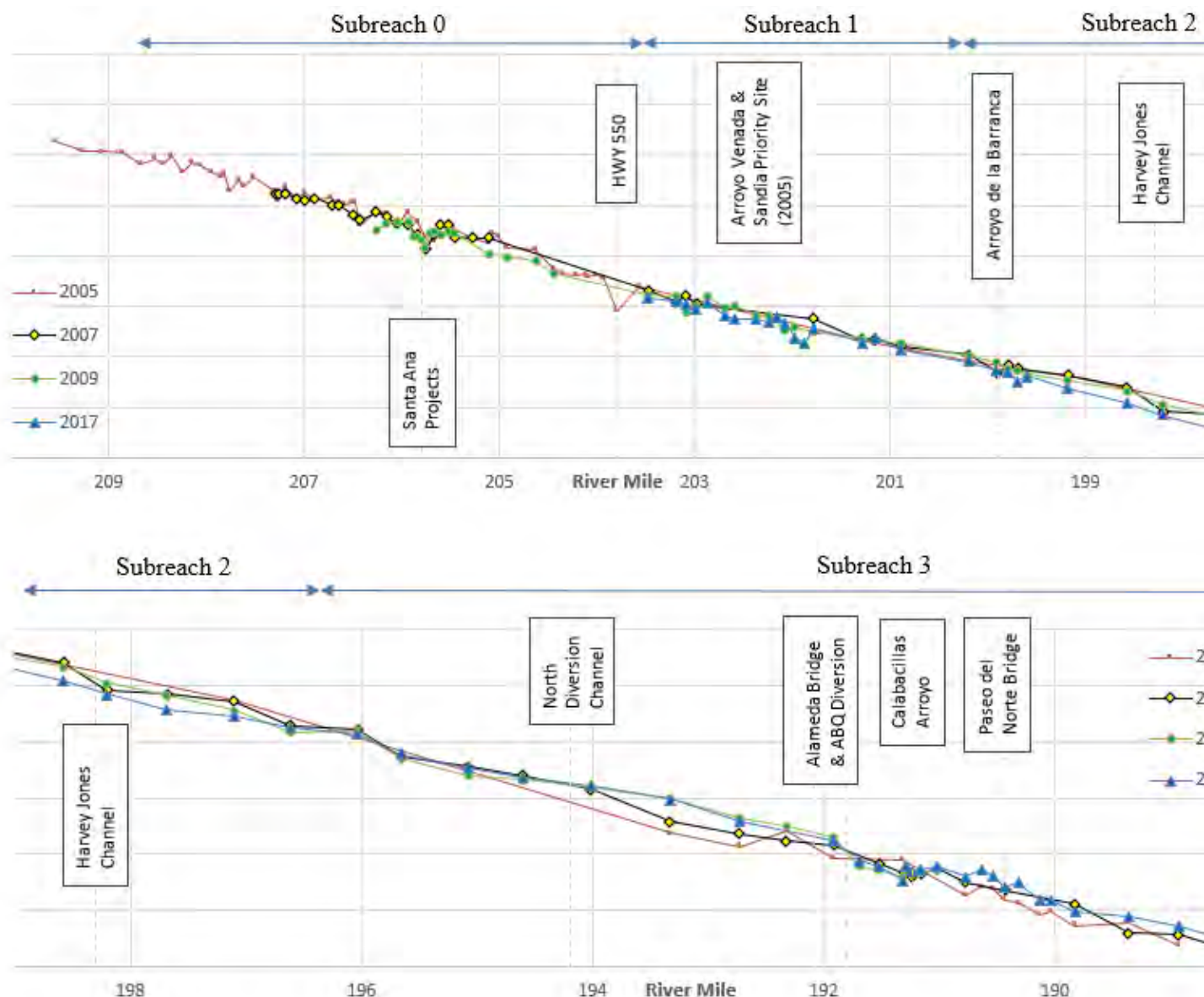


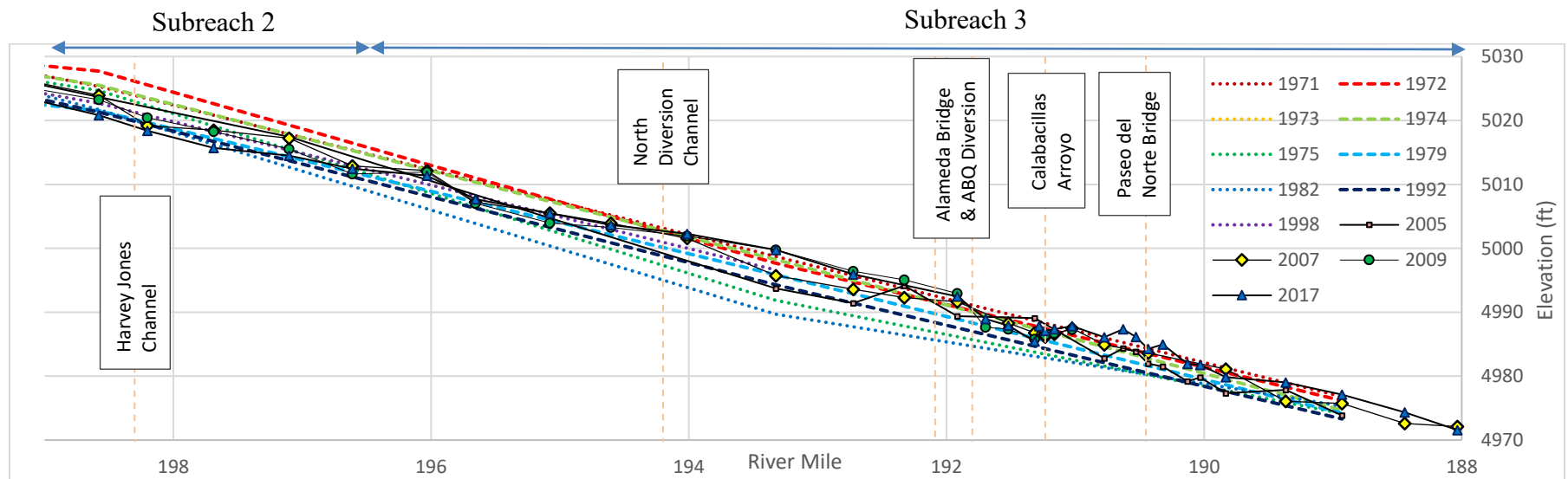
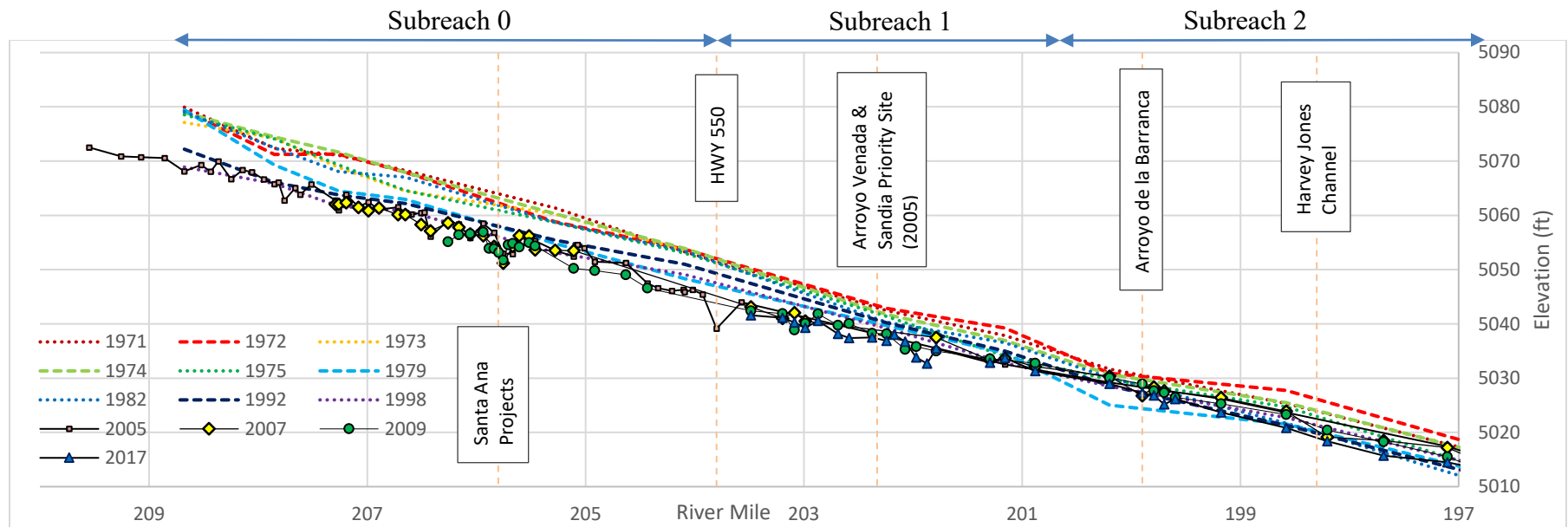
Figure 3). Thalweg elevations, station and elevation pairs, and locations of the right and left banks were recorded for all the river cross sectional rangelines.

Cochiti rangeline (CO-lines) data was compiled for years following the closure of Cochiti Dam, from 1973 to 1998. In Figure 3, these data are shown as a dashed line. The most current data captures particular rangelines throughout the reach, represented with solid black lines, to easily discern the most recent data to the more generalized historical data. It should be noted that the data for Subreach 0 was collected at a different time than for Subreaches 1 to 3. The rangelines of Subreach 0 are located on the Pueblo of Santa Ana, and the Pueblo conducted its own hydrographic data collection that was independent from data collected by Reclamation's contractors. For Figure 3, Subreach 0 data for 2007 was actually collected in 2008; data for 2009 was collected in 2010 (Santa Ana Pueblo data). These data were consolidated with Subreaches 1-3 for these respective years.

As visible from the Angostura Diversion Dam to approximately the AMAFCA North Diversion Channel, the reach has been degrading over time. Ephemeral tributaries such as the Arroyo de la Barranca, the Arroyo Venada (across from the Sandia Pueblo Priority Site), and the Calabacillas Arroyo have effects on the channel thalweg, as indicated by depressions in the thalweg corresponding with degradation occurring downstream of arroyos. Depending on the arroyo's sediment characteristics and hydrologic transport efficiency and the magnitude of events that occur in its watershed, arroyos affect the Rio Grande as a local grade control. The signal of an arroyo input is indicated in a longitudinal profile with areas that have a flat slope upstream and a steeper slope downstream.

The location of the 2017 repair of some bendway weirs at Sandia Priority Site is downstream of Arroyo Venada. The location of the emergency repair of Corrales Siphon in 2016 is downstream of Arroyo de la Barranca. Around 2015, grade control structures were placed within the Calabacillas Arroyo upstream of its confluence with the Rio Grande to prevent degradation of the arroyo, and thus reduced arroyo sediment loads into the river that slowed down the growth of the sediment deposit at the confluence of the arroyo and the river as well as scour of the river thalweg downstream of the arroyo.

Structures such as the AMAFCA North Diversion Channel and the Alameda Bridge act as local vertical and lateral controls, respectively. Throughout the past decade the thalweg profile has been stable in the vicinity of these structures. In the period between 1971 and 1998 generally the entire reach was degradational; this trend continued up to 2017 below the Harvey Jones Channel to the end of sub-reach 2 near River Mile 197. Downstream of the AMAFCA North Diversion Channel the current thalweg elevations are comparable to 1973 elevations. Effects to the river bed in Sub-reach 3 from immediately upstream of San Juan Chama Surface Diversion Dam to the North Diversion Channel are evident in the profile with rise in the bed and a flattening of the slope. This channel spanning diversion facility was installed in 2008.



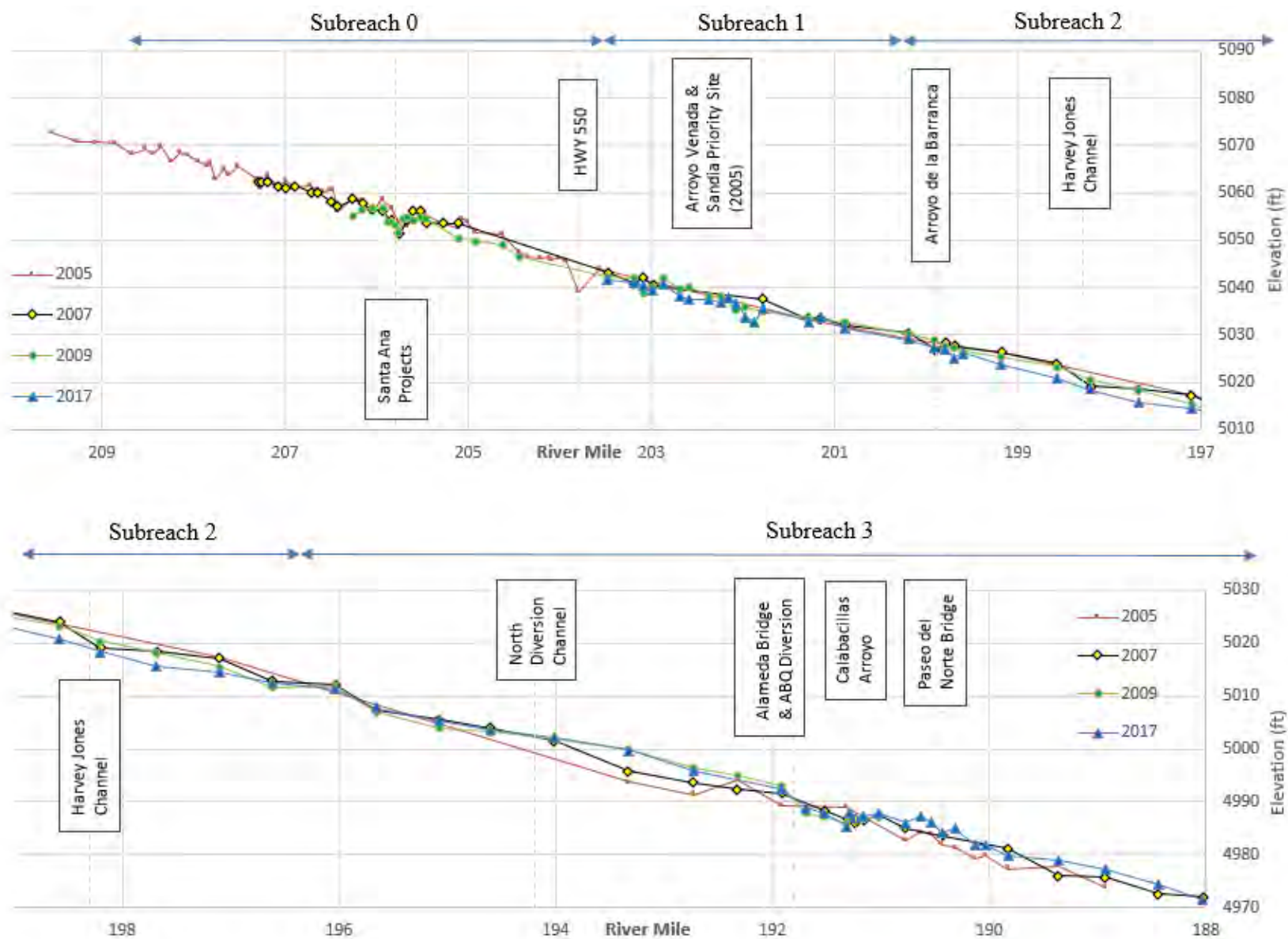


Figure 3 Longitudinal profile of the Rio Grande within the reach.

3.2 Slope

From the 1930s to the 1970s, the reach trend of aggradation occurred between the riverside levees, causing the channel and floodplain contained within the levees to become perched by as much as five feet (Reclamation 2007). With the construction of upstream dams, most significantly between 1950 and 1973, the sediment supply of the reach decreased, and the channel began to degrade with the main sediments transported being coarser (MEI 2002). The channel degradation is associated with an average of 3-5 feet channel incision from 1962 to 2001 (Reclamation 2007). The slope in the reach is generally decreasing since 1972 (MEI 2002).

Table 2 Historical mean thalweg slopes modified from Tetra Tech (2013).

Year	1962	1972	1992	2002	2012*
Subreaches 1-3 Average Slope (ft/ft)	0.00093	0.00095	0.00094	0.00090	0.0012
Year	1971*	1979*	1983*	1992*	2005*
Subreach 0 Average Slope (ft/ft) from CO-24 to CO-29	0.00092	0.00113	0.00094	0.00087	0.00092

* Not from Tetra Tech 2013.

Hydrographic data was evaluated, and the thalweg and water surface elevations for recent years were summarized from contractor data collected for Subreaches 1 to 3. Further analysis is presented in Section 3.2.2. Subreach 0 data was not available for coinciding years with Subreaches 1 to 3. Selected available data from CO-lines encompassing Subreach 0 was averaged to be included in Table 2. Further analysis is presented in Section 3.2.1.

3.2.1 Slope Analysis for Subreach 0

For Subreach 0, the thalweg slope was evaluated based on Cochiti (CO) rangeline data. A distance weighted averaged slope was calculated based on the elevation of the thalweg divided by the distance between each rangeline calculated from 2012 River Miles. Major features within the subreach, in reference to CO-lines, are shown in Table 3. Major events, such as the closure of Cochiti Dam in 1973, the change in operations at Jemez Canyon Dam in 2001, and the installation of grade control structures from 2001 to 2005 on the Pueblo of Santa Ana has marked impacts on the slope within Subreach 0.

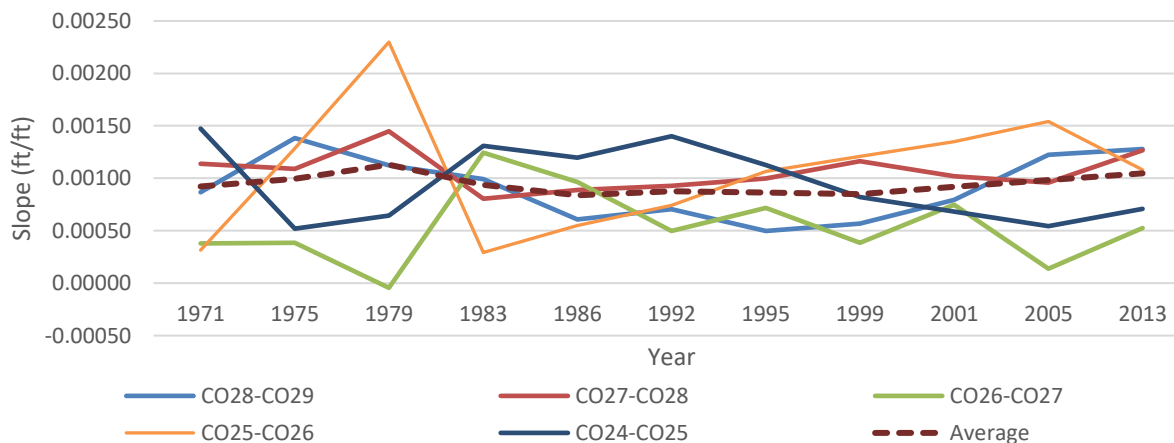


Figure 4 Slope analysis of Cochiti (CO) rangelines in Subreach 0.

An interesting observation is that the average slope throughout Subreach 0 remains relatively constant throughout the changes in the reach at CO-lines. This is likely due to features maintaining grade at Angostura Diversion Dam, the Jemez confluence, and the grade control structures in the river channel. Data analyzed in Figure 4 is represented as a longitudinal profile in Figure 5.

Table 3 Features in Subreach 0, relative to CO-lines.

Feature	Location	Year Built
Cochiti Dam	CO-0	Closure in 1973
Jemez Confluence	Between CO-24 and CO-25	Jemez Dam closure in 1950s; sediment operations change in 2001 to pass more sediment
Gradient Restoration Facility (GRF) #1	Between CO-24 and CO-25	2001
GRF #2	Immediately downstream of CO-27	2005
Santa Ana Projects	Between CO-27 and CO-28	Bar-lowering in 2005, bendway weirs in 2014
GRF #3	Immediately upstream of CO-28	2005

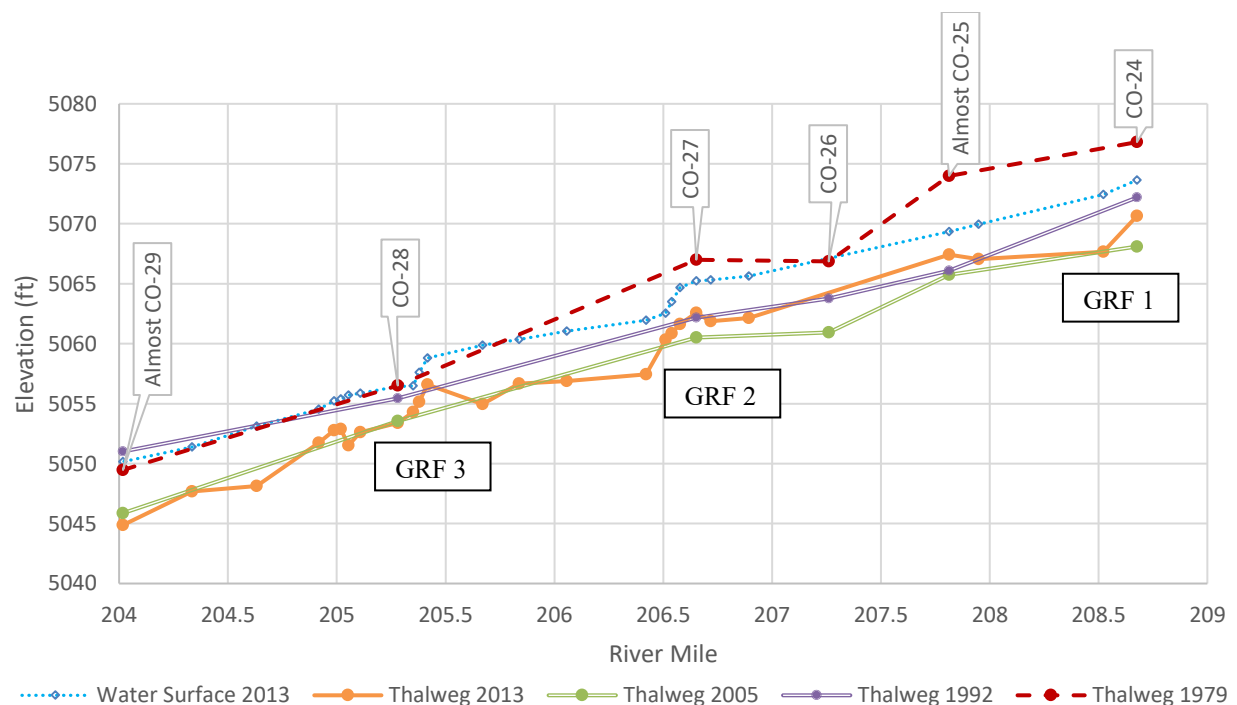


Figure 5 Longitudinal profile for Subreach 0 thalweg in notable years.

3.2.2 Slope Analysis for Subreaches 1 to 3

The slope was evaluated by the most upstream station available and the most downstream station using hydrographic data and 2012 River Mile locations (

Figure 6). Anomalies were identified, based on the difference of station-by-station slopes and their magnitude relative to the reach average. An anomaly of note is in 2004 in Subreach 1, where there was a steep gradient between BB-304.8 and BB-305, around Bernalillo Priority Site. According to recent aerial photography, this area is a location where there appears to be thalweg adjustment and river straightening. It was also observed that there was a negative thalweg slope between CA-7 and CA-11 in 2017 of Subreach 3; this location coincides with the Calabacillas Arroyo.

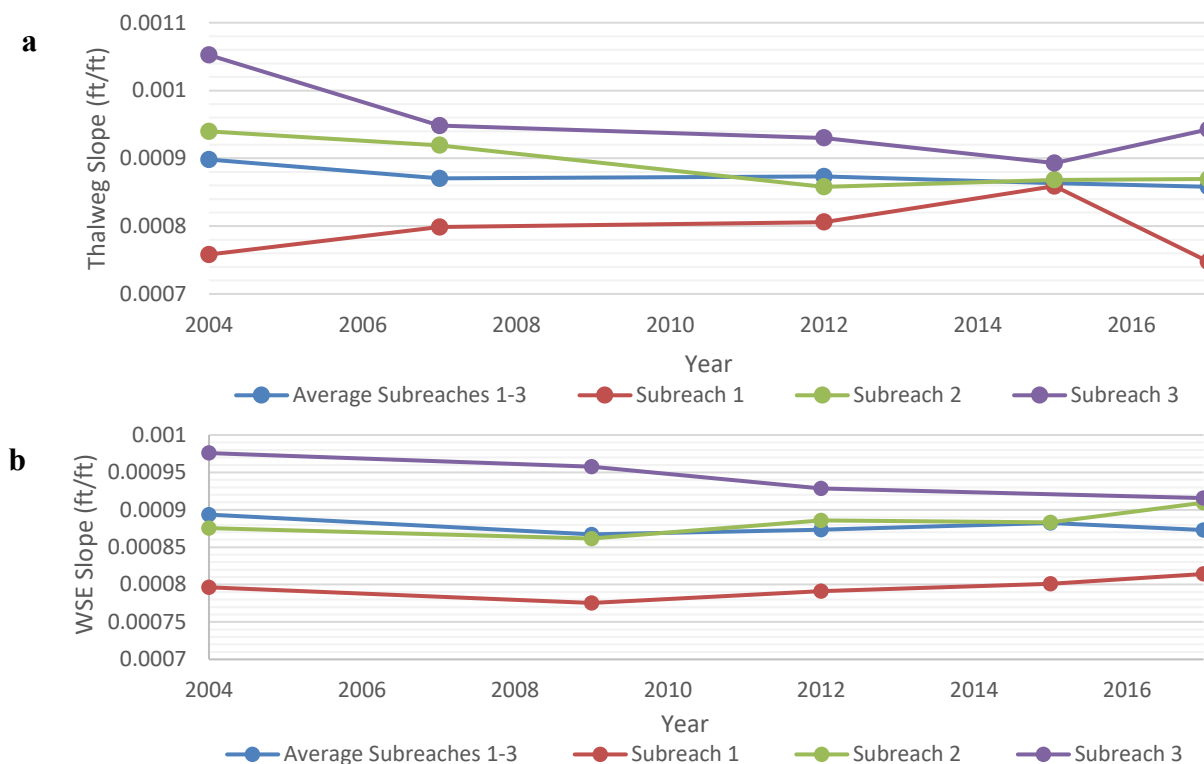


Figure 6 Reach distance weighted, averaged thalweg slope results from hydrographic data collection for a) the thalweg profile; and b) the water surface elevation.

Table 4 Reach averaged thalweg slope results from hydrographic data collection for the thalweg profile and the water surface elevation for Subreaches 1, 2, and 3, as presented in

Figure 6.

Year	Approximate Dates of Data Collection	Approximate USGS 08330000 Discharge at Albuquerque gage	Average Thalweg Slope (ft/ft)	Average Water Surface Elevation Slope (ft/ft)
2004	August 9 to August 14	350 cfs	0.00090	0.00089
2009	September 28 to October 3	350 cfs	0.00087	0.00087
2012	January 9 to 20	550 cfs	0.00087	0.00087
2015	August 4 to 20	700 cfs	0.00086	0.00088
2017	August 15 to 24	400 cfs	0.00087	0.00087

3.3 Channel Width

Generally, the channel width has been decreasing since the first recorded surveys in 1918. The trends in geometry show that width has reduced from 1,338 feet in 1918 (MEI 2002) to about 465 feet in 2011 (Tetra Tech 2013). From 1949, the channel narrowing can be attributed to the reduction of sediment supply and flood control operations which have reduced the peak flows (Makar and AuBuchon 2012). Federal activities to channelize the river in the 1950s to 1970s involved the installation of steel jetty jacks by Reclamation and USACE and reduced the width of the channel to 550-600 feet wide. Channel width was further reduced as dredging and bar mowing and removal practices that had occurred from 1962 to 1992 ceased (MEI 2002), allowing main channel sand bars to become stable with vegetation (Tetra Tech 2013). Narrowing is exacerbated by the reduction of sediment supply due to Cochiti and Jemez Canyon Dams, located on the main stem and the major tributary of the Jemez River, respectively. The jetty fields, designed for the trapping and storing sediment and debris, no longer function as designed and instead the jetty jacks act to stabilize the vegetation growth on depositional features (Makar and AuBuchon 2012).

Table 5 shows the non-vegetated channel width values over time and their analysis source. Figure 7 shows the channel width values graphically. The MEI analysis for 1918 channel width consisted of evaluating the active channel width on contour maps at every 2-foot drop in elevation. The 1972 and 1992 analysis consisted of evaluating the active channel width at every fifth rangeline (MEI 2002). Tetra Tech's 2013 analysis measured the active channel width at certain rangelines, and the Reclamation analysis measured the channel width at the same rangelines to coincide with methods applied by Tetra Tech (2013). Channel width includes all parts of the active channel, including non-vegetated side channels.

Table 5 Average Channel Width Values for the HWY 550 to Montañó reach

Year	Average Channel Width (feet)		
	MEI Analysis (2002)	Tetra Tech Analysis (2013)	Reclamation Analysis (2018)
1918	1338		
1962		736	
1972	577	624	
1992	519	554	
2001		506	
2011		465	451
2014			349
2018			267

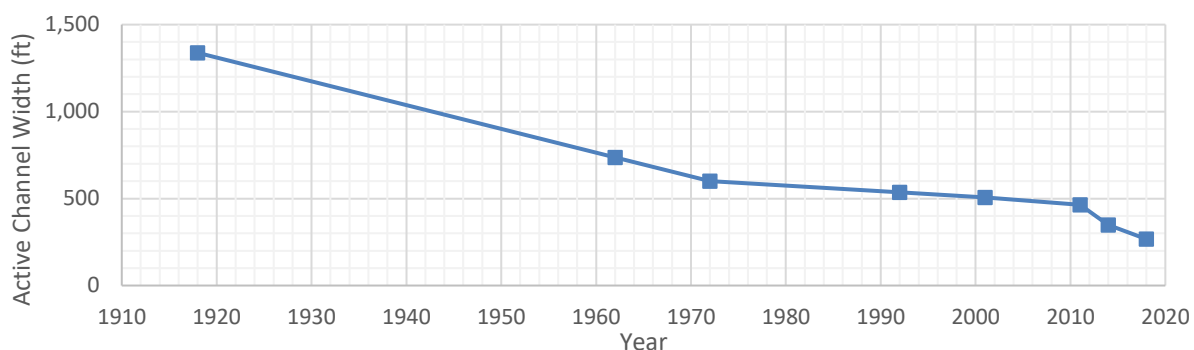


Figure 7 Average Active Channel Width from HWY 550 to Montañó Bridge

Due to the planform's progression to a single thread channel (See Section 3.5.2), this reach has many side channels that have been abandoned and are now inaccessible to the active channel; however, these side channels are still lower in elevation than the surrounding floodplain. The channel width decreased below 600 feet between 1972 and 1992; 600 feet coincides with the width between the frontline channelization jetty jack lines. This channel width coincides with current limitations imposed by the Interstate Stream Commission's policy on habitat restoration, in order to not incur excess depletions.

3.3.1 Levee Width Analysis

Levee infrastructure has been instrumental in establishing stability in the Rio Grande Valley agriculture and communities, as the levees provide some protection from high discharge events of the Rio Grande. Historical records of levees used as flood protection can be found in the late 19th century, and records of drainage ditches predate the 17th century (Berry and Lewis, 1997). These records indicate that the levees were not necessarily engineered geotechnically to reduce seepage or withstand particular flows, as many were created out of excavated spoil from drain excavation. In some areas, floodwater trajectories were so unlike the river's active channel that the levee locations near bends were especially worrisome for potential failure (Berry and Lewis, 1997). In 1928, the MRGCD Chief Engineer's *Official Plan* indicated that existing drains would be used to reduce the amount of disturbance during district-wide construction. These ditches

were adapted with engineered design and head gates (Berry and Lewis, 1997). The combination of drains and levees provide flood protection from river flows for surrounding agricultural fields as well as increases in the supply of water for irrigation.

A levee width analysis was completed to determine the average, maximum and minimum distances between levees or other riverside infrastructure. The distances between the 2012 river centerline and the levees/infrastructure were also evaluated. The purpose of this analysis is to determine the degree of freedom for the river planform.

Using ArcMap 10.4.1 and Reclamation aerial imagery from 2012, the levees were outlined for the reach from HWY 550 to Montañó. In some areas there was infrastructure closer to the river than the levees; specifically the Albuquerque Bernalillo County Water Utility Authority (ABCWUA) water treatment plant and the AMAFCA North Diversion Channel. The levee delineation followed this infrastructure instead of following the levees in these areas. Levees are present for this reach except for the right side of the river upstream of Corrales Siphon. For this area lacking levees, a line was drawn with an approximate 100-foot buffer to the closest structures, which were typically residential developments. For the upstream-most half mile before the HWY 550 bridge, the houses on the right side of the river are extremely close to the active channel and a 100-foot buffer was not possible; thus, the delineation was created along the right channel bankline.

A centerline between the levees was created and perpendicular lines were generated every 150 feet along the levee centerline. These perpendicular lines were clipped at the levee delineation and their lengths were all determined. From this data set, the minimum, maximum, and average distance between the levees was determined and a graph was created to show the distance between levees for the entire reach (Figure 8).

From HWY 550 to Montañó, the maximum width between levees was 2,704 feet in an area located just upstream of the AMAFCA North Diversion Channel. The minimum width for the entire reach was 600 feet at rangeline BB-306, located in the Bosque Encantado Neighborhood. The average width was 1,609 feet. For the reach that has levees on both sides (Corrales Siphon downstream to Montañó) the minimum width was 810 feet at the ABCWUA Diversion Dam, and the average width was 1,707 feet.

Although Figure 8A shows that the distance between levees would support the average channel width in Figure 7, Figure 8B shows that in certain areas widening the channel would not be a viable river maintenance or habitat restoration alternative as the distances from the centerline to the levees do not allow further expansion. These areas include the right levee by the Alameda Footbridge and by Corrales Siphon, or the left bank in the Bosque Encantado neighborhood. Discussion of meander bends in relation to the levee locations continues in Section 3.5.3.

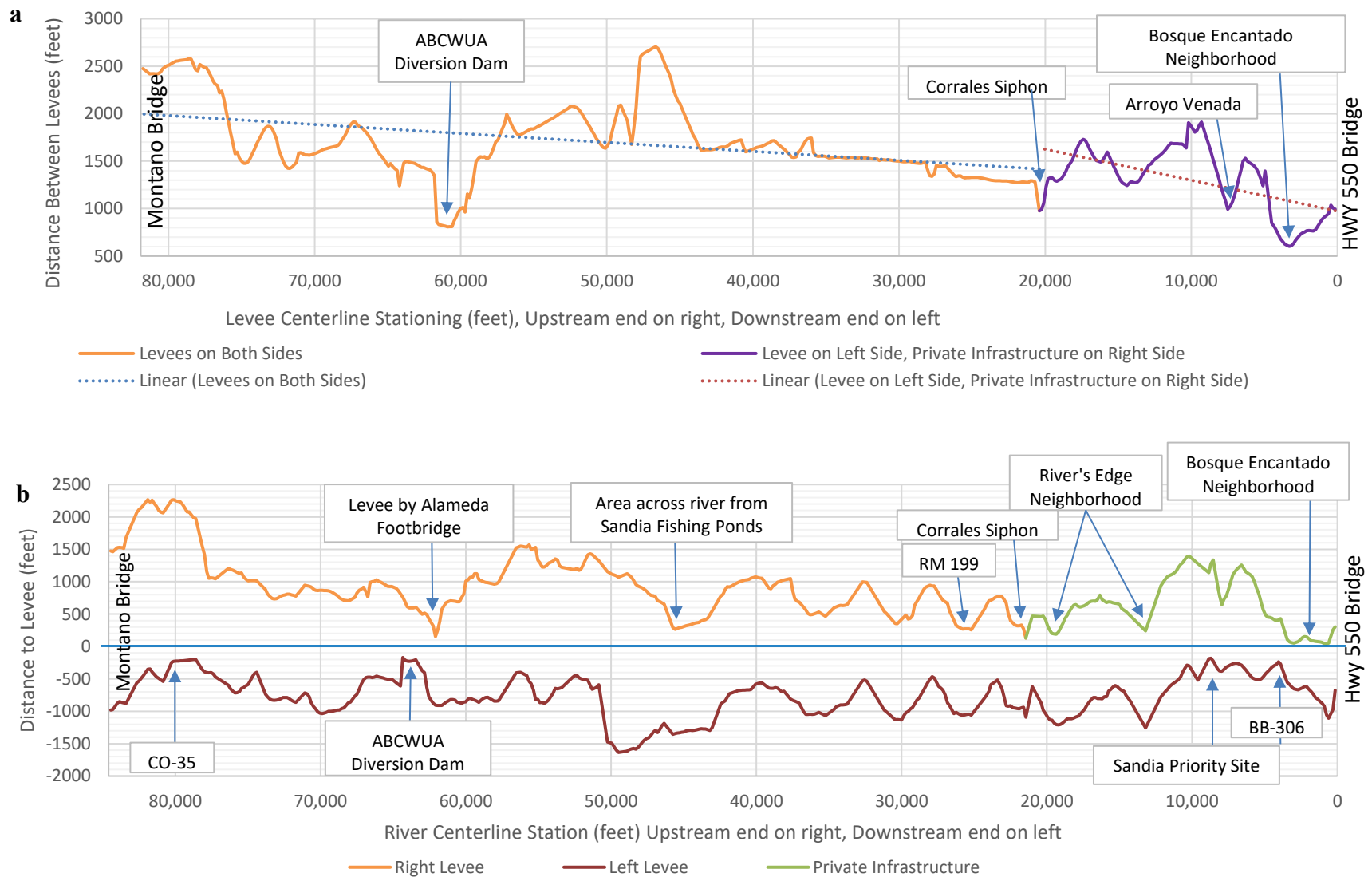


Figure 8 (a) Total perpendicular distance between levees and (b) Distance to right and left levees from the 2012 Rio Grande centerline

3.4 Sinuosity

Channel sinuosity is a ratio of the length of channel in comparison to the valley length. Changes in sinuosity are created by bank erosion or encroachment of vegetation (Makar and AuBuchon, 2012). The underlying driver is the river balancing its sediment transport capacity with the sediment supply; if the bed material is more stable than the bank material and the river has excess sediment transport capacity, then bank erosion will occur.

Aerial photography from 1972, 1992, 2006 and 2016 was visually inspected in ArcGIS. The measuring tool was applied to determine the valley length in between levees for each subreach, and then the river length throughout. It should be noted that in 1972 it appears there was much more significant flow at that time in comparison to following years. This may cause sinuosity measurements to be less significant because the high-discharge flow path tends to overbank and hide the sinuous nature of the active channel.

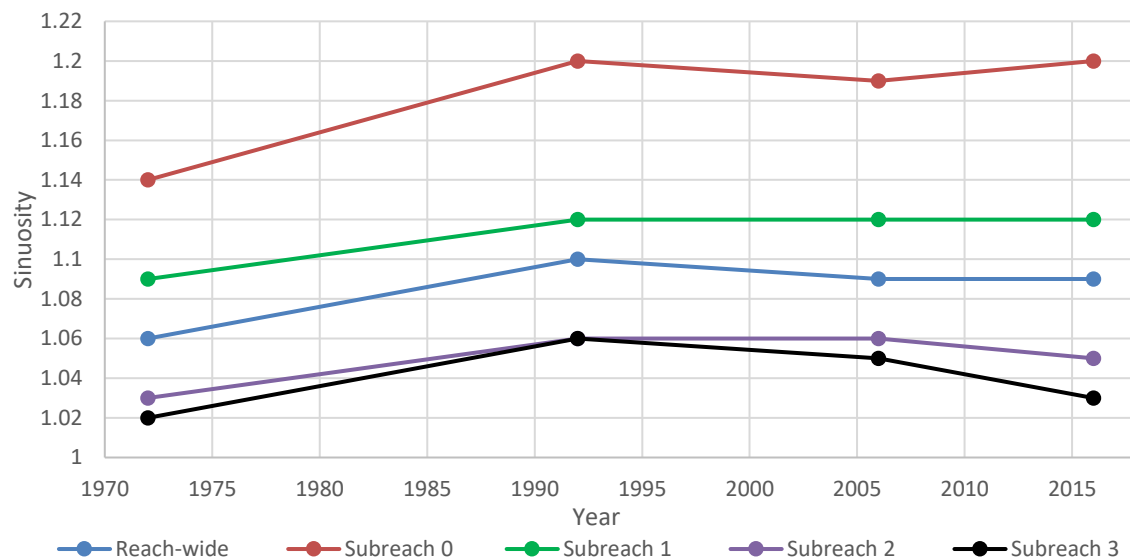


Figure 9 Sinuosity for the study reach; values presented in Table 5.

Subreach 0 from Angostura dam to HWY 550 is the most sinuous of the study reaches, and it is increasing in its sinuosity over time. Subreach 1 has appeared to have reached a dynamic equilibrium, with the total sinuosity of the reach not varying much from year to year within the study period. Lower subreaches are showing trends of reducing sinuosity, indicating that the river is straightening in some sections and may be becoming less braided.

Table 6 Sinuosity of the reach from HWY 550 to Montaña Bridge (modified from Tetra Tech 2013; Reclamation 2017).

Year	Reach-wide	Subreach 0	Subreach 1	Subreach 2	Subreach 3
1972	1.06	1.14	1.09	1.03	1.02
1992	1.10	1.20	1.12	1.06	1.06
2006	1.09	1.19	1.12	1.06	1.05
2016	1.09	1.20	1.12	1.05	1.03

The sinuosity and channel geometry trends identified in Subreach 0 corroborates with Schumm's model (discussed in 2.1 Channel Geometry and Hydraulic Parameters). However, for the lower reaches the sinuosity is decreasing, which does not corroborate with Schumm's model. Schumm's model projects an increase in sinuosity with the observed decrease in discharge and sediment discharge. This may indicate that sediment sources or hydrologic regimes are not consistent throughout the Reach.

3.5 River Planform

Sediment and hydrologic regimes determine planform changes that are occurring in the Reach. Massong et al. (2010) developed a planform model for the Middle Rio Grande that describes the systematic changes that the Middle Rio Grande experiences due to sediment supply and transport capacity. The changes in the planform are observable by the development, erosion, and stabilization of sand bars; the establishment of vegetation along the banks; and the singular or braided channel flow paths. The aerial photography collected by Reclamation was observed alongside traced active channel planforms of the Rio Grande (Figure 10). Rangeline by rangeline evaluation is conducted in Section 3.5.1.

Up to the 14th century, the Middle Rio Grande was an aggrading, braided channel with ephemeral riparian and wetland habitats, meaning that habitat is generated, destroyed and replaced by natural river progression (Crawford et al., 1993). More recently, the river is responding to anthropogenic controls including lateral controls such as levees and jetty fields and grade controls such as dams and channel-spanning river structures. The river will likely continue to adjust as its sediment and hydrologic regimes are affected by flow reduction and regulation through dams. It is apparent that the river planform in 1918 (no aerial photography available, planform shapefile was assessed) had been confined by a levee by 1935 upstream of CO-32 and from CA-11 to CR-443. In 1935, after levee placement, the channel had varied widths and vegetated islands throughout, the river banks had sandy bars attached. Compared to later years, the river was wide in 1935, but had narrowed its planform compared to 1918. The channel was dredged in the 1930s by MRGCD to maintain a narrower floodway (Reclamation 2007).

The stabilization of a narrow channel was induced by jetty jack installation and levee construction between 1953 and 1975 (MEI 2002). At the time, the channel was generally a multi-thread channel with shifting, non-vegetated sandbars. Also contributing to the change in sediment and hydrologic regimes were seven upstream dams that were placed in the river reach from the 1950s to 1976; especially significant for this reach is the installation of Cochiti and Jemez Canyon Dams (Tetra Tech 2013). The effects of the installation of the dams are observed with the channel continuing its narrowing trend into 1962, with a predominately a single threaded channel persisting from BB-306 to CR-355.

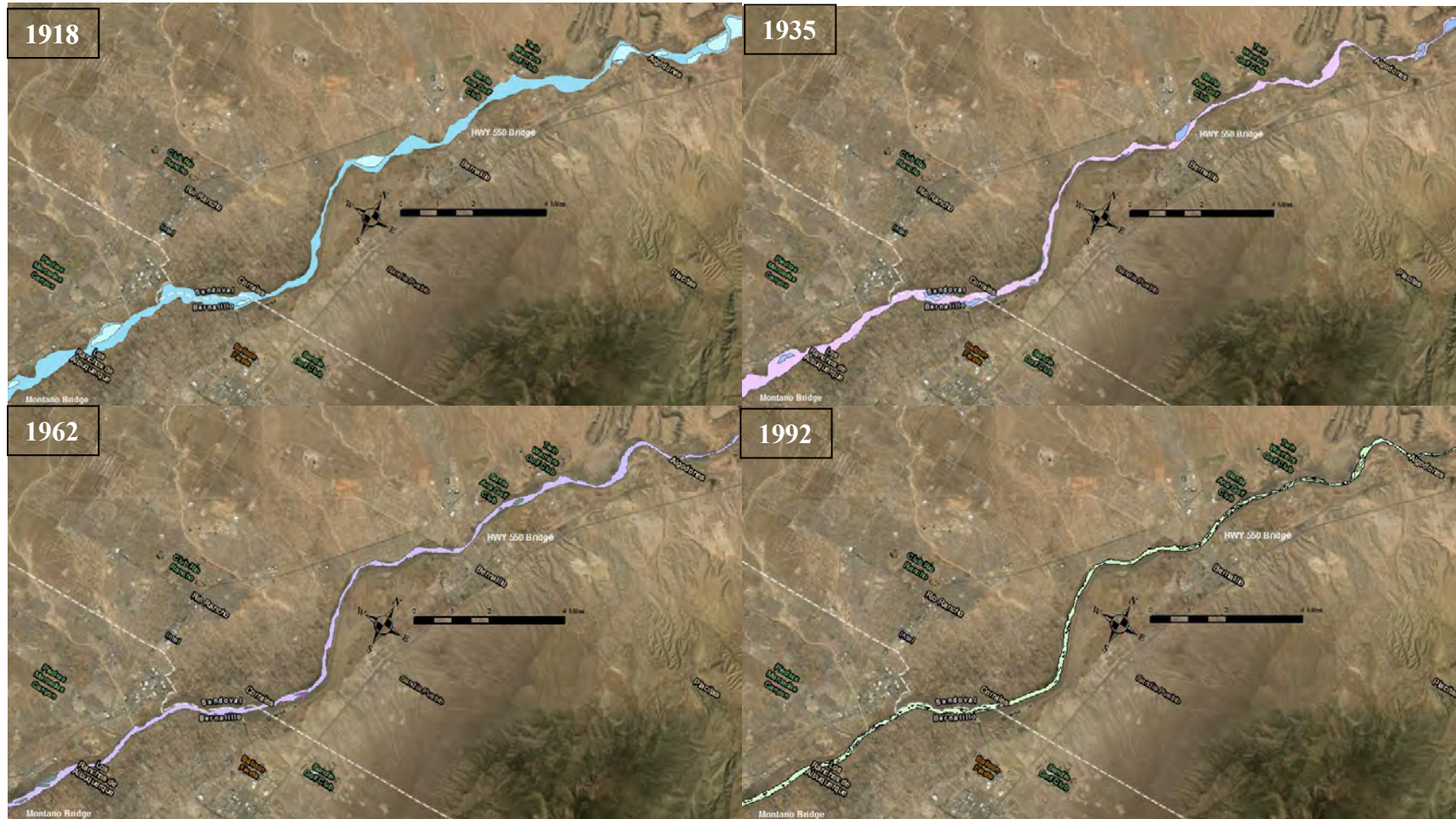


Figure 10 Planform outlines for the reach in various years. River narrowing and reduction of large in-stream features such as islands and attached sandbars is evident for the entire reach from Angostura to Montañito Bridge.

By 1972 the channel planform was narrow and uniform in width, with bars near the bank being the dominant deposition pattern. These side bars were non-vegetated at the time. In 1985, aerial photography shows a significant adjustment (aerial photography is not available for the entire reach), with many sandbars populating in the river channel, creating several flow paths. The river planform remained narrow and uniform in comparison to 1972 data. The channel width persists from observations in 1992 and 2006, but the surface area of sandy bars generally increases and becomes established with vegetation (especially in 2006).

In recent years, there has been an adjustment of the river from a multi-threaded channel to a single-threaded channel. As seen in Figure 10, starting at Arroyo de la Barranca (BB-338), a single thread became apparent by 1992, continuing 1.5 miles downstream to the Harvey Jones drainage channel. By 2002, HWY 550 (near BB-300.1) to Arroyo de la Barranca was transitioning to single-thread. In 2005, the vegetated islands in the reach of Harvey Jones Channel to the North Diversion Channel became attached to the banks, furthering the channel's transition to single-thread. By 2009, the transition to single thread is complete down to the North Diversion Channel.

3.5.1 Meander Bends and Erosion

In general, from 1918 to 1992, the rates of lateral movement of the Rio Grande in this reach had decreased and bank stability had increased; however, lateral migration has increased downstream of arroyos. Lateral stability can be found in areas where the channel is single thread and where there are areas of geological control preventing lateral migration. A recent study (Richard, 2000) showed that the flow energy and the planform most affected variance in the migration rates of the Rio Grande. Migration rates increase with increases in flow energy, sinuosity, and channel width (Richard, 2000). As seen in aerial imagery taken between 1935 and 1972, the entire Angostura Diversion Dam to Montañito reach was a multi-thread or braided channel with shifting and non-vegetated sandbars. In 2002, the aerial imagery shows that the area from HWY 550 to the Arroyo de la Barranca transitioned from multi-thread to single-thread at low flow regimes. Meander bend geometry was evaluated in-depth from aerial photography from 2006 and 2016. The ability to evaluate the bend geometry in the braided planforms was problematic and some analysis was omitted for particular bends or when the reach was transitioning to a straight reach, as wavelength and belt width was measured relative to the next downstream bend. The measure tool in ArcGIS was used to determine the distance between bend apexes (wavelength), the distance from the inside of a bend the inside of a preceding bend on the opposite river side (belt width), and the arc length for each bend. A circle tool was used to estimate the radius of curvature for each identified bend. General observations show that the wavelength is decreasing (except for Subreach 2), and belt width is decreasing. This conforms to Schumm's model as it applies to this reach. The number of bends per subreach generally increased from 2006 to 2016, except for Subreach 3 where there was a decrease.

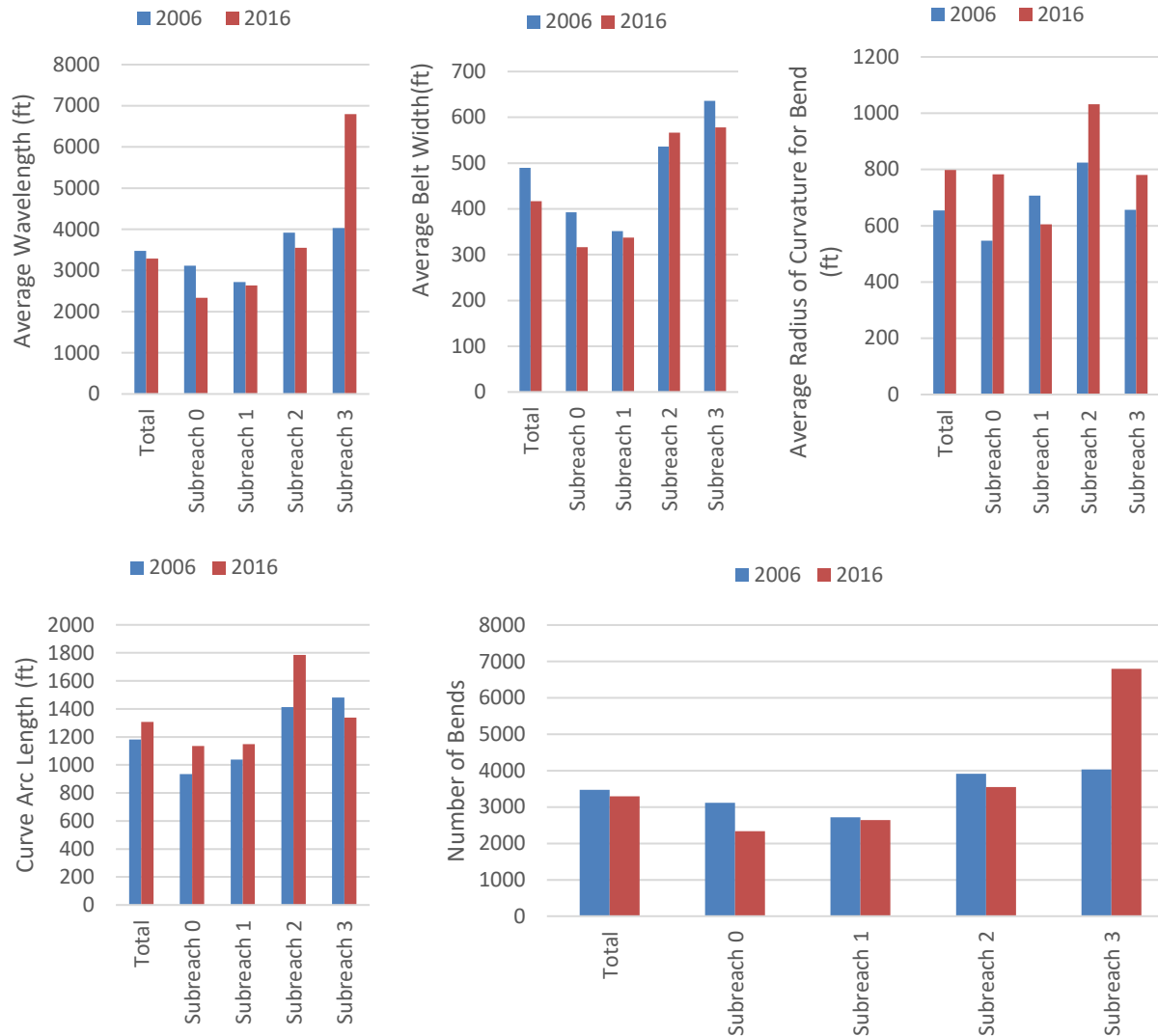


Table 7 Results of averaged meander bend geometry observations for the study reach. Figures representing these data are shown above.

2006	Total Reach	Subreach 0	Subreach 1	Subreach 2	Subreach 3
No. of Bends	49	18	7	9	14
Wavelength (ft) (min; max)	3470 (1260; 7560)	3110 (1260; 7560)	2720 (1700; 5800)	3920 (2270; 5470)	4030 (1920; 5350)
Belt Width (ft) (min; max)	490 (100; 1351)	390 (100; 1351)	350 (100; 530)	540 (220; 753)	640 (330; 890)
Radius of Curvature (ft) (min; max)	650 (100; 2010)	550 (170; 910)	710 (100; 1690)	820 (275; 2010)	660 (170; 1250)
Arc Length (ft) (min; max)	1180 (300; 2860)	930 (440; 2250)	1040 (300; 1980)	1410 (640; 2960)	1480 (665; 2220)

2016	Total Reach	Subreach 0	Subreach 1	Subreach 2	Subreach 3
No. of Bends	53	21	12	13	7
Wavelength (ft) (min; max)	3290 (300; 12380)	2330 (300; 7600)	2640 (1070; 4700)	3550 (1030; 6220)	6800 (2110; 12380)
Belt Width (ft) (min; max)	420 (100;950)	320 (100; 650)	340 (200; 630)	570 (160; 950)	580 (350; 790)
Radius of Curvature (ft) (min; max)	800 (290; 2745)	780 (325; 2745)	610 (280;1350)	1030 (350; 2435)	780 (315; 1250)
Arc Length (ft) (min; max)	1310 (520; 3310)	1140 (520; 2260)	1150 (700; 2460)	1790 (720; 3310)	1340 (670; 2770)

In addition to the geometry results shown in Table 7, the radius of curvature of the identified bends were compared as a ratio to the width local to the bend location. For ratios around 2 to 3, river bend geometry is oriented in a way that indicates lateral migration is most likely (Heo et al, 2008). The bends in 2016 were evaluated, and it is indicated that the following range lines are near bends that have a propensity for migration:

Table 8 Meander bend locations with a propensity for lateral migration according to Heo 2008.

MI	Nearest Rangeline	Description	Radius of Curvature - RC (ft)	Width -W (FT)	Rc/W
210.0	N/A	below Angostura Dam	325	150	2.17
209.1	N/A		410	150	2.73
208.2	TA-249	near Jemez Confluence	345	110	3.14
207.2	TA-263		400	160	2.50
206.2	TA-275		370	160	2.31
206.0	TA-276	upstream of RM 205.8	380	140	2.71
202.1	BB-315	near Sandia Priority site	280	100	2.80
202.0	BB-316		330	100	3.30
201.3	BB-323	coincides with Willow Creek area	460	160	2.88
199.9	BB-338	across from Arroyo de la Barranca	350	180	1.94
197.7	CR-361		545	160	3.41
197.1	CR-367		620	220	2.82
196.6	CR-372	southernmost end of most confinement by levees (see Figure 17)	515	170	3.03
195.1	CR-388		375	170	2.21
193.3	CO-34	near Sandia Pueblo access	315	200	1.58

Many of these locations correspond with currently existing monitoring locations and priority sites. This demonstrates an objective method for reach analysis to identify potential river maintenance conditions, especially in locations that are confined by public infrastructure.

The 2006 and 2016 comparative analysis was used to identify locations of measured change. Using aerial photography, and the above described geometry analysis, areas of change were investigated. Meanders were evaluated assuming that the river's tendency is to move as a single channel with bends in alternating directions. Areas where the river's planform transitions to a straight or braided channel are problematic in this evaluation. In 1992, the river in this reach is predominantly braided; therefore meander geometry was not captured, but the aerial photography was included in the discussion to give context of the developing trends.

Once the meander geometry, wavelength and belt width were identified and measured from historical aerial photography in 2006 and 2016, the belt width was plotted and compared (Figure 11). To facilitate in comparison, bends to the east or river left had their width demonstrated with negative (-) values. Areas of divergence between 2006 and 2016 are indicated as number 1-8 in Figure 11, and will be further discussed. General observations from Figure 11 indicate that in the upstream portion of the reach, from Angostura Dam to around RM 200/Arroyo de la Barranca, the belt width is generally uniform, with a width of less than 500 feet and the meander wavelengths are consistent. Downstream from near Corrales Siphon (RM 200) towards Montañño Bridge, the belt widths increase, and the meander wavelengths also increase. Also, the locations of bends change dramatically between 2006 and 2016 relative to upstream geometry measurements. Description of mechanisms for these changes are described in the following figures.

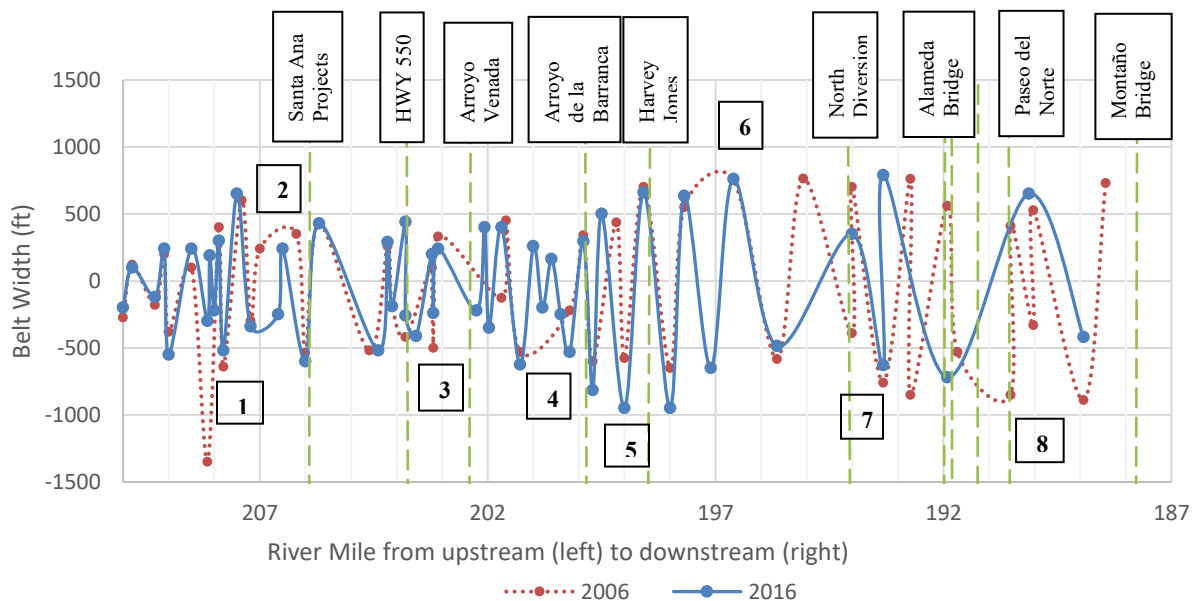


Figure 11 Meander belt widths based on location in the reach; negative values indicate bends on river left. Areas of divergence (1-8) are discussed in following figures.

Areas of divergence, or change, from 2006 to 2016 were identified:

1. Near CO-25 (RM 208)
2. Near TA-275 (RM 206)
3. Near BB-316 (RM 202)
4. Near CO-32 (RM 200)
5. Between BB-345 and CO-33 (RM 199)
6. Near CR-367 (RM 197)
7. Near CR-400 (RM 194)
8. CO-34 to CR-441 (RM 193 to RM 190)

The migrations are demonstrated in Figure 12 through Figure 16.

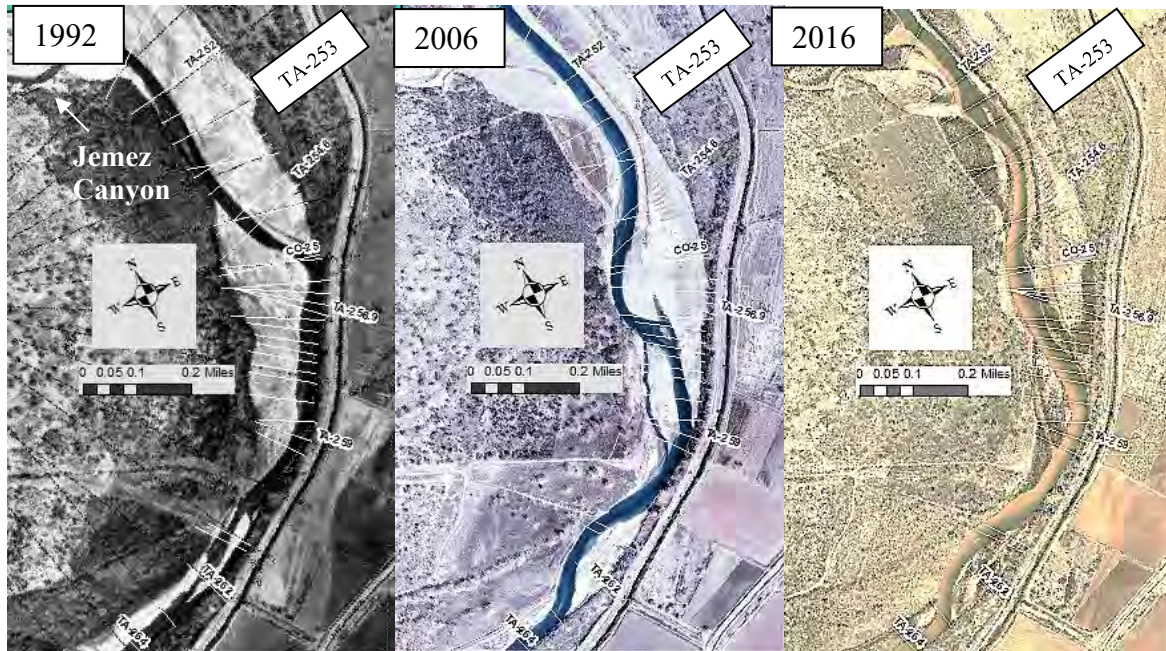


Figure 12 Bend changes near CO-25 to opposite active channel bank; bend formation shown near TA-253 in 2016. This is below Jemez Canyon. (1)



Figure 13 Near TA-275. Bend migrating downstream, resulting in a tighter meander, as the river's left bend at TA-277.5 is fixed, this location coincides with Santa Ana Projects. Yellow arrow is approximately at the same position in all images. (2)

Divergence 4 at CO-32, near RM 200 indicates a similar trend to Divergence 2 (Figure 13), where the bend is migrating downstream. The migration at Divergence 4 occurs both above and below Arroyo de la Barranca at BB-338, where the bend below has migrated since 1992. Both of these divergences (2 and 4) show that the river runs straight along the river right edge of the active channel planform as if the Rio Grande would have a smooth bend with a wider belt width if it had not reached some rigid bankline control.

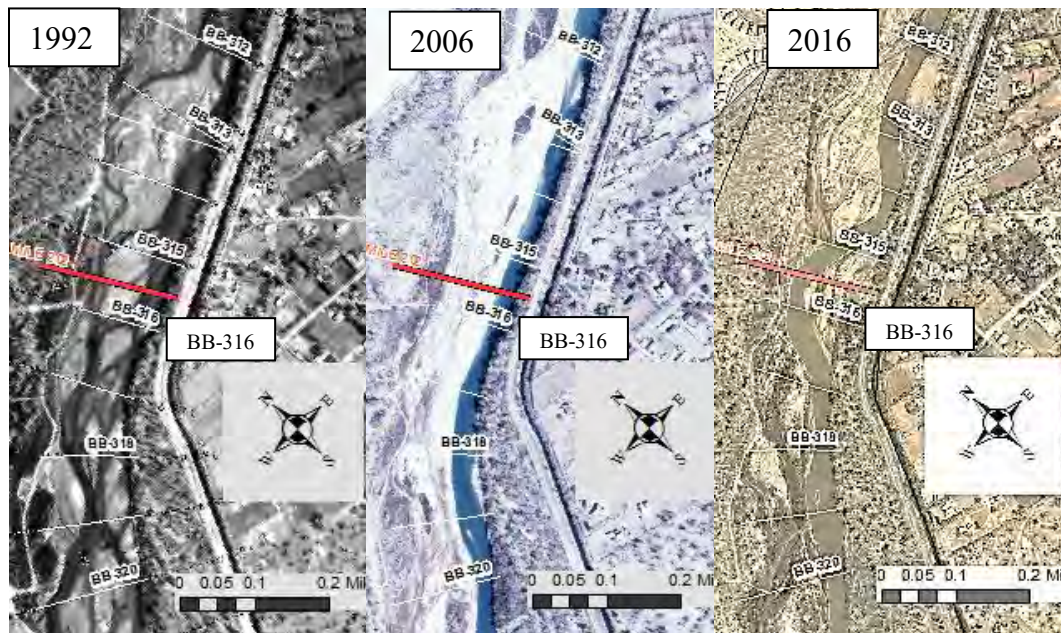


Figure 14 Near BB-316, where the braided planform shifted to a straight channel by 2006, and then Reclamation construction activities in 2008 constructed bends with bendway weir structures at Sandia Priority Site, with an inception of non-constructed bends at BB-313 and BB-318 as well. (3)

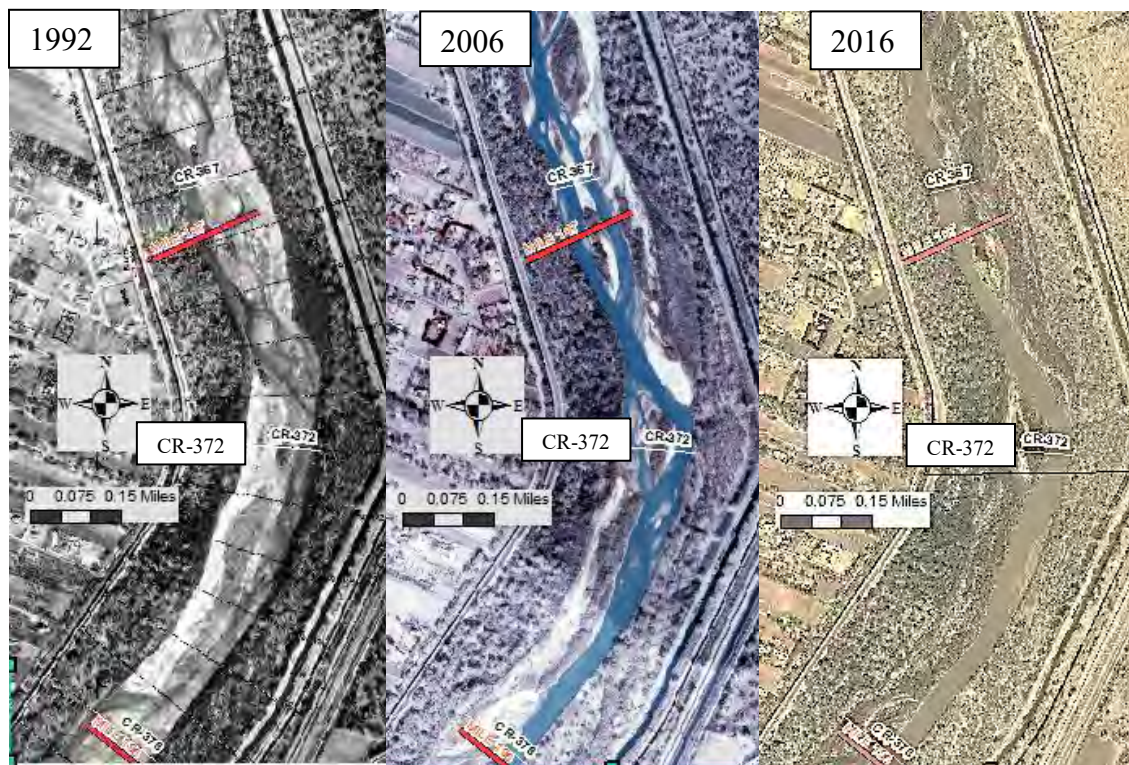


Figure 15 Planform change near CR-372, from braided and dynamic planforms in 1992 and 2006 to the singular channel in 2016. (6)

The changes at CR-400 near the AMAFCA channel, above Paseo del Norte Bridge at the CA-rangelines near RM 191 (7), below Paseo del Norte Bridge to CR-441 (8) are of a similar progression as that identified near CR-372 (Figure 15). The encroachment of vegetation in the form of bank attached bars and islands is evident in these portions of the reach, and the braided channel planform with non-vegetated sand bars has progressed to a single channel. From 2006 to 2016 imagery, the area above Paseo del Norte Bridge shows disconnection of the Calabacillas Arroyo and vegetation stabilizing in the area.



Figure 16 Changes in the planform above Alameda Bridge, where the braided planform has become established by vegetation, and connected side channels in 2016 imagery. (8).

Similar to the changes above Alameda Bridge in Figure 16, Divergence 5 between BB-345 and CO-33 or around RM 199 shows the stabilization of non-vegetated sand bars with vegetation. In the case of Divergence 5, however, high flow channels present in 2006 have become vegetated in 2016.

General trends throughout the reach includes the inception of bends, the migration of bends downstream, vegetation encroachment setting the active channel and side channels in place or causing the loss of side channels and connections to arroyos, and also the installation of in-stream features such as bendway weirs that confine or restrict channel lateral movement.

To demonstrate the tendency for meandering bends to necessitate intervention to protect infrastructure, the levee width analysis (Section 3.3.1) was combined with the belt width analysis from earlier in this Section 3.5.1. From this representation (Figure 17), it is apparent near HWY 550 (RM 203.8) and from Corrales Siphon (near RM 200) to the AMAFCA North Diversion Channel (RM 197) some of the meander bends' belt width poses a threat to the levees (i.e the meander belt width doesn't fit within the levees). RM 199, already identified by Reclamation as a future river maintenance site is located within this area. Other locations to note are above Alameda Bridge (RM 193.5), ABCWUA Plant (RM 192), and RM 190 which is mid-way between Paseo del Norte and Montaña Bridges. It should be noted that the river downstream of RM 194 has areas that have not yet progressed to a single thread channel (Section 3.5.2) and are currently in a braided planform stage. These areas are not expected to be threatened by rapidly moving migrating bends until the areas have transitioned to a single thread channel.

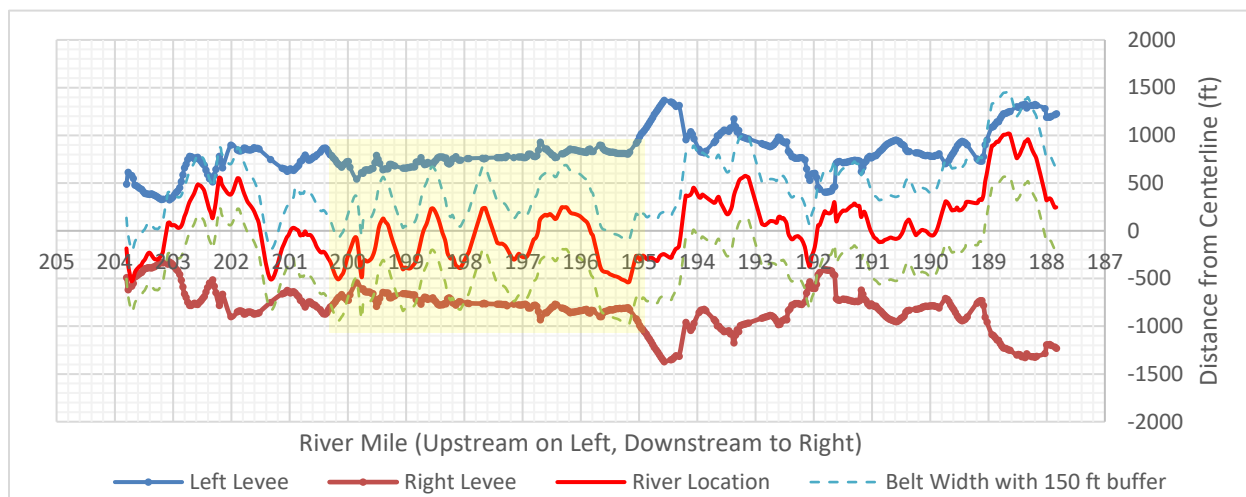


Figure 17 2016 Belt width analysis combined with levee distance analysis. Area in commentary highlighted in yellow.

3.5.2 Meandering Planform Evolution Analysis

In 2010, Massong et al. defined planform stages common to the Middle Rio Grande. These stages and their short descriptions can be seen in Figure 18 and Table 8. The reach from Angostura Diversion Dam to Montañño Bridge was classified according to these planform stages for the years 1949, 1962, 1972, 1992, 2002, 2012, and 2016. Excess transport capacity was identified as the planform evolution pattern for this reach. Aerial imagery and cross section plots were used in the planform classification. New evaluation criteria were created to increase objectivity when classifying the rangelines (see Table 9). These guidelines only applied when cross section plots were available, making the more recent years (post 1972) have more information for analysis. Generally, it was observed that the reach conforms to Massong's Migrating Planform model (M4-M8) due to the excess transport capacity in this portion of the Middle Rio Grande.

Table 9 Definition of Massong Planform Stages and additional Evaluation Criteria used in the analysis (Massong et al., 2010).

Planform Evolution Stage	Definition	Evaluation Criteria
Stage 1	Mobile sand bed channel	
Stage 2	Sand islands stabilized with vegetation	The lowest point or thalweg of the channel to the high point of the island was more than four feet.
Stage 3	Areas between the vegetated islands and the banks partially fill in with sand, creating side channels	Stage 2 criteria plus the channel on one side of the island(s) was much smaller or more filled in than the other side of the island(s) (the smaller, filled-in portion of the channel is considered a side channel).
Stage M4	The side channels fill in more fully and vegetate, the active channel becomes single thread. Flat channel bed	The side channel is more than three feet higher than the main channel. The channel bottom was relatively flat.
Stage M5	The natural bends in the channel carve out a thalweg.	If the single thread channel bottom was not flat but showed presence of a thalweg.
Stage M6	Erosion occurs creating bend and channel migration	When aerial imagery showed the active channel bends eroding between years.
Stage M7	Cutoff channels form on the inside of the bends	Not observed in this analysis.
Stage M8	The cutoff channel becomes the main channel	Not observed in this analysis.

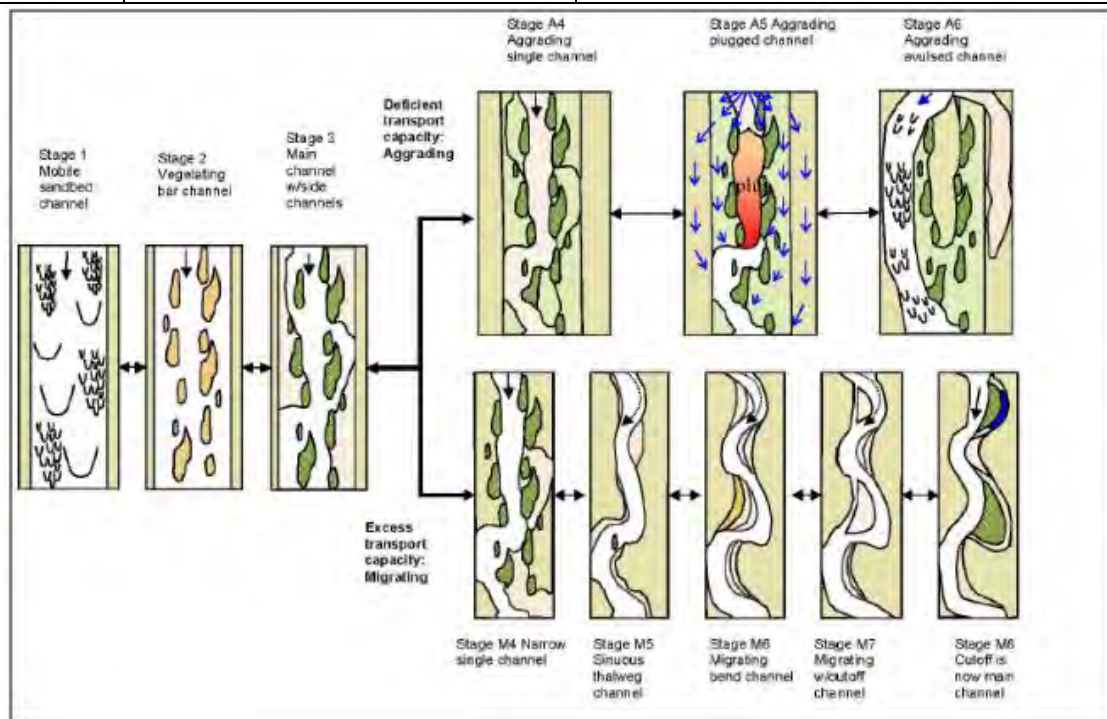


Figure 18 Middle Rio Grande planform cycle model (from Massong et al., 2010).

The planform evolution stage classification was performed at each rangeline of the study reach. Figure 19 shows the planform classification for years 1949, 1962, and 1972. An 8-period moving average was used to demonstrate overall trends in each year. The Middle Rio Grande at this time can be classified predominantly as Stage 1: a mobile sand bed channel. There were a few vegetated islands throughout the reach which were classified as a Stage 2: vegetating bar channel.

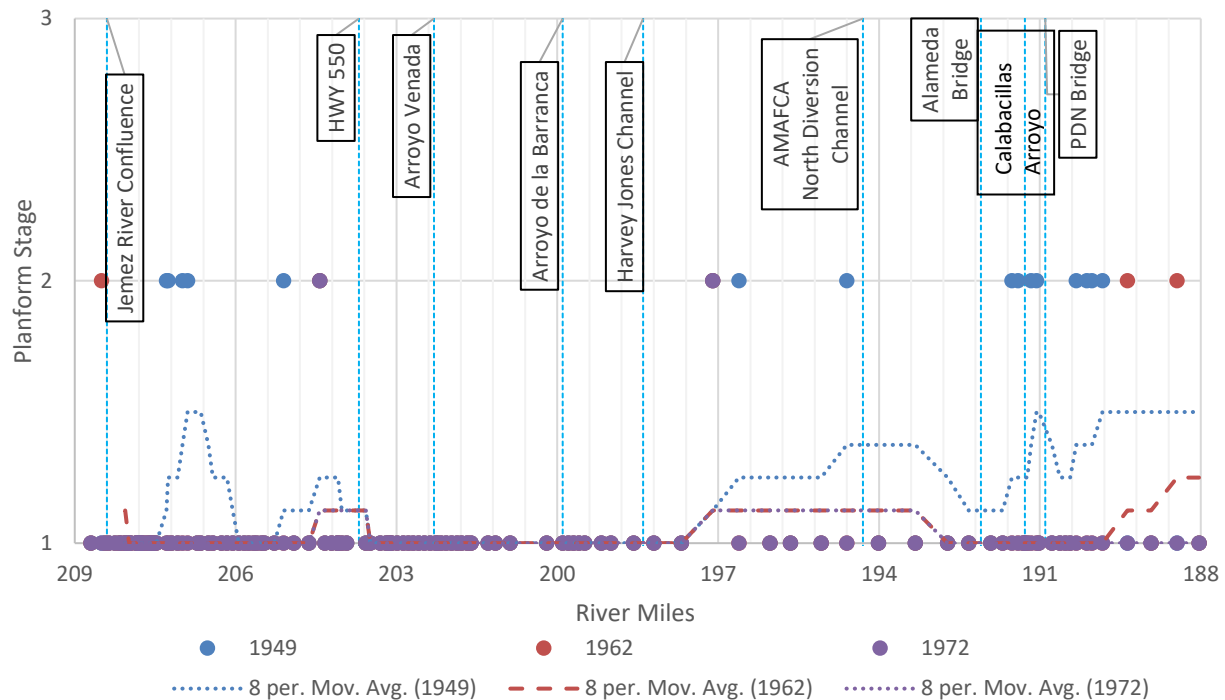


Figure 19 Planform classifications for the Angostura Dam to Montano Reach.

Figure 20 shows the planform classification for years 1992, 2002, 2012, and 2016. An 8-period moving average was used to demonstrate overall trends in each year. The changes in planform from cross section to cross section would not be expected to have an algebraic relationship, but the moving average shows areas where generally the planform stage is similar or changing relative to surrounding cross sections.

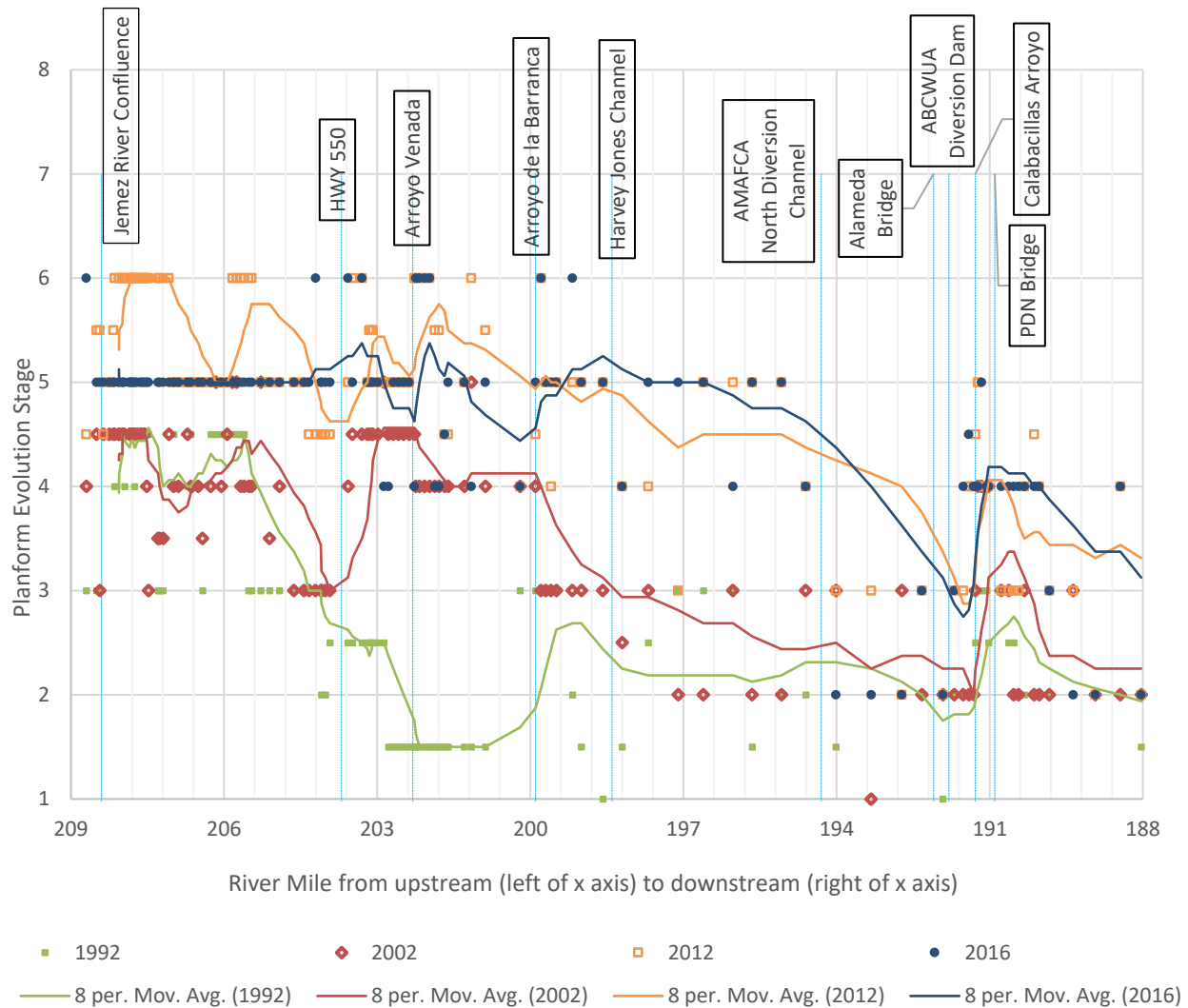


Figure 20 River planform analysis for the Angostura Dam to Montañito Reach, 1992 to 2016.

In each of these years, the Massong planform evolution stage has progressed at the upstream end before the downstream progresses, as if the planform progression is increasing and migrating downstream. The point of transition between a single thread channel (Stage M4 and above) to a multi-thread channel (Stage 3 and below) moves downstream for each of these years. In 1992, the planform transition point is approximately half way between the Jemez River and HWY 550. In 2002, the transition point is approximately at the Arroyo de la Barranca. In 2012, the transition point from Stage 3 to Stage M4 is approximately at the AMAFCA North Diversion Channel. In 2016, the transition point may have moved downstream of Montañito Bridge, with a few multi-thread channel areas present immediately downstream of the AMAFCA North Diversion Channel.

The factors contributing to the changes in the Middle Rio Grande over time can be classified as both natural and anthropogenic. Anthropogenic factors after 1949 include the placement of jetty jacks, channelization, bendway weirs, and bank armoring resulting from the placement of in-stream structures (see Section 3.6.1 for Bed Material); construction and operations at dams upstream and within the study reach; and land use changes such as urbanization or changed

grazing practices. Natural factors could include changes in peak flow and sediment concentration due to climate change and landscape changes. Generally, the changes cause the channel to be confined and allow for vegetation encroachment. The channel planform may be so restricted laterally that the planform cannot complete bend migration (M6) and progress to cutoff channels (M7).

3.5.3 Vegetation Changes

Before the 14th century, the Middle Rio Grande Valley was an aggrading, braided channel that would generate ephemeral riparian and wetland areas. As agriculture and other anthropogenic factors took hold of the river valley, river flows were diminished. Cottonwood willow forests were reduced by agriculture, tree harvesting and water diversion; livestock grazed on the riparian vegetation, contributing to watershed erosion and sediment loading in the Rio Grande. Wetland resources disappeared or became confined to man-made drains. Drains were required in the Middle Rio Grande Valley due to high groundwater levels causing high alkalinity in the soil. The high groundwater levels were the result of channel aggradation. Vegetative species such as Russian olive, salt cedar, white clover and summer cypress were introduced in the riparian zones (Crawford et al, 1993). With water operations regulating discharges, the duration of low flows persists for longer periods than historically. The increased duration of water in the river system aquatic habitat, but also aids in the encroachment of vegetation to the active channel leading to further narrowing (Makar and AuBuchon 2012).

Observations of the changing vegetative landscape of the floodplain in the reach can be made from National Wetlands Inventory in Figure 21 for 1935 and 1989. In 1935, the Rio Grande valley was surrounded by agricultural land, with swaths of wetland, range and cottonwood. From the vegetative maps, the planform also contained many sandbars that extended beyond the active channel and into arroyos. In the figure, for 1989, it is apparent that the valley has been further developed for urban use and agriculture. The presence of wetlands is much less persistent, and there are fewer sandbars dominating the river course way and outside the active channel footprint.

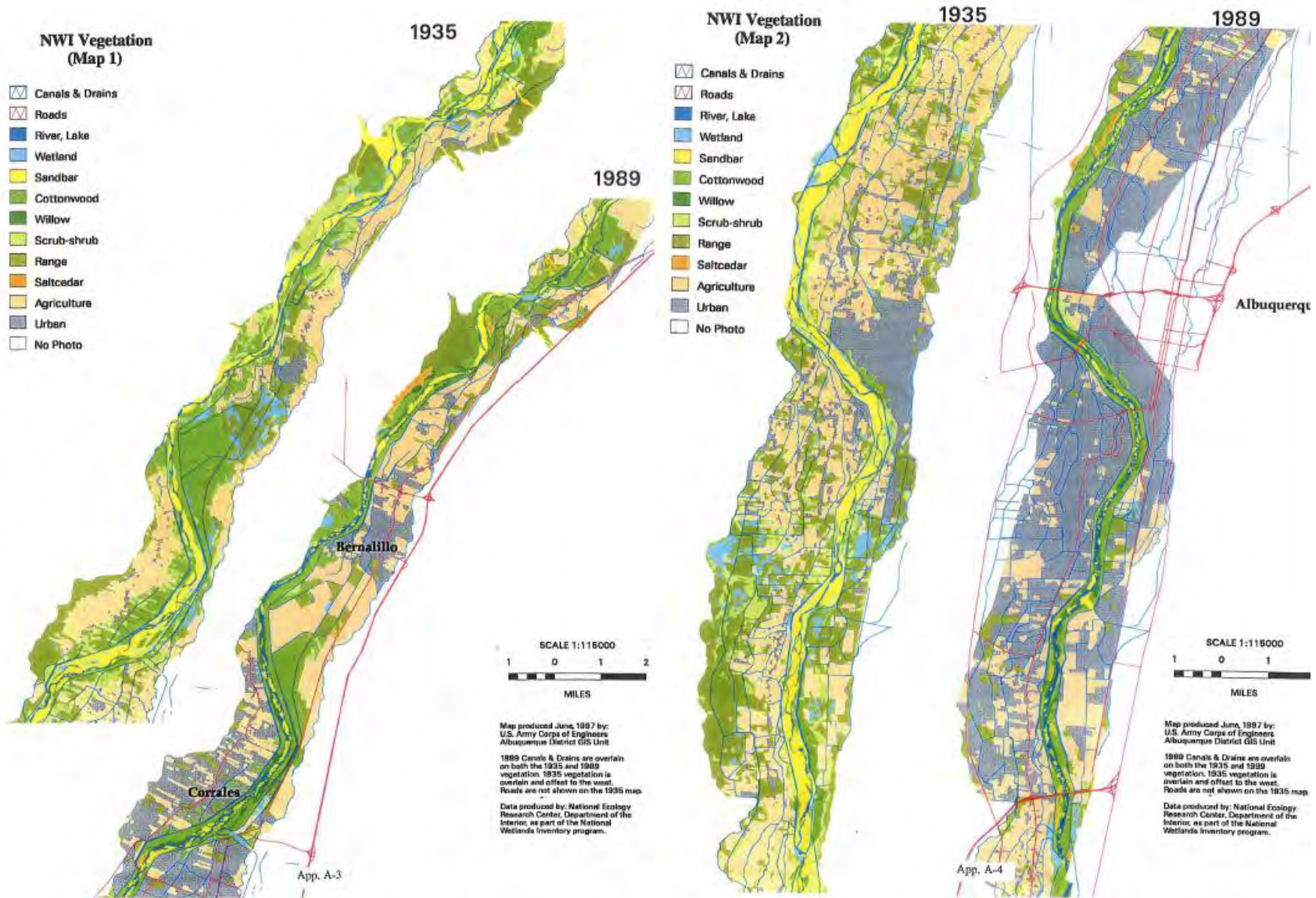


Figure 21 National Wetlands Inventory Program maps produced by Army Corps of Engineers for Berry and Lewis (1997).

From 1962 to 1992, the channel was maintained with pilot channeling and debris clearing resulting in the removal of sand bars (MEI 2002). This prevented bars from becoming stable with vegetation. However, since the practice ended, sand bars have formed and have stabilized with vegetation.

Trends are shown in Table 10 and Figure 22, where the active channel area has decreased persistently from 1962 to 2017. The area of vegetated islands and bars have varied, as the islands and bars have likely attached and vegetated to the point of being inaccessible by normal channel discharges. In 2017, it was evident that most islands persisted in the lower part of the reach, Subreaches 2 and 3.

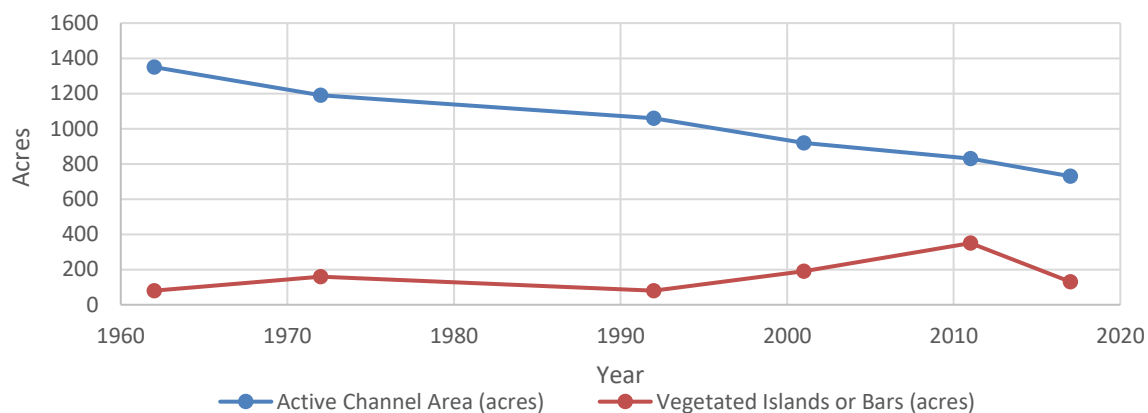


Figure 22 Active channel area in comparison to vegetated islands and bars, modified from Tetra Tech (2013).

Table 10 Digitized active channel area in comparison to vegetated islands and bars, modified from Tetra Tech (2013).

	1962	1972	1992	2001	2011	2017
Active Channel Area (acres)	1350	1190	1060	920	830	730
Vegetated Islands or Bars (acres)	80	160	80	190	350	130
Percent Coverage of Active Channel Area by Islands or Bars	6%	13%	8%	21%	42%	18%

The reduction in both active channel area and vegetated island or bars in 2017 indicates that more areas are becoming upland terraces.

3.6 Sediment Supply and Transport

The presence of reservoirs and other sediment control measures in the arroyos and floodplain and changes in land use are drivers in the reduction of sediment loads for much of the Rio Grande (Makar and AuBuchon, 2012).

3.6.1 Bed material

In general, due to flood control facilities, the median bed material size in the Middle Rio Grande has increased while the sediment supply has decreased (Makar and AuBuchon 2012). Makar also

observed that from Cochiti Dam to the northern part of Albuquerque, the bed material of the channel is dominated by gravel. These gravel deposits influence the bed elevation at many flows and are transported as bed load. The reach from northern Albuquerque down to Isleta Diversion Dam is transitioning to a gravel-dominated bed (Makar and AuBuchon 2012).

Bed materials samples collected from 2003 to 2016 were compiled for this analysis. Table 11 shows average grain size distribution. It also shows the temporal and spatial variability of the surficial bed material samples with the majority of the median bed material sizes being gravel for all the subreaches. A sample D_{50} size of 2 mm is the demarcation between sand and gravel.

As one travels downstream through the reach, there is a general trend of decreasing grain size. There are transition zones, at TA-275 (RM 208), CO-30/BB-340 (RM 200), at CA-1 (RM 192), and at CA-9 (RM 191). These zones of change are surrounded by constructed in-stream features: Santa Ana Projects, Corrales Siphon, Alameda Bridge, and Montañño Bridge respectively.

Table 11 Summary of changes in bed material size for varying subreaches of the Rio Grande.

Year	Location	D₃₅	D₅₀	D₈₄
2003	BB-301 to BB-318 (2/3 of subreach 1)	< 1 mm	<1 mm	12 mm
2005	CA-12 to CO-35 (small section of subreach 3)	< 1 mm	2 mm	4 mm
2009	BB-301 to CA-9 (subreaches 1 & 2 and 1/2 of subreach 3)	2 mm	5 mm	17 mm
2012	BB-301 to CR-462 (subreaches 1 to 3)	2 mm	5 mm	21 mm
2014	BB-301 to BB-345 (subreach 1 and 1/2 of subreach 2)	7 mm	13 mm	30 mm
2016	CO-30 to CR-462 (1/2 of subreach 1 to subreach 3)	<1 mm	1 mm	10 mm

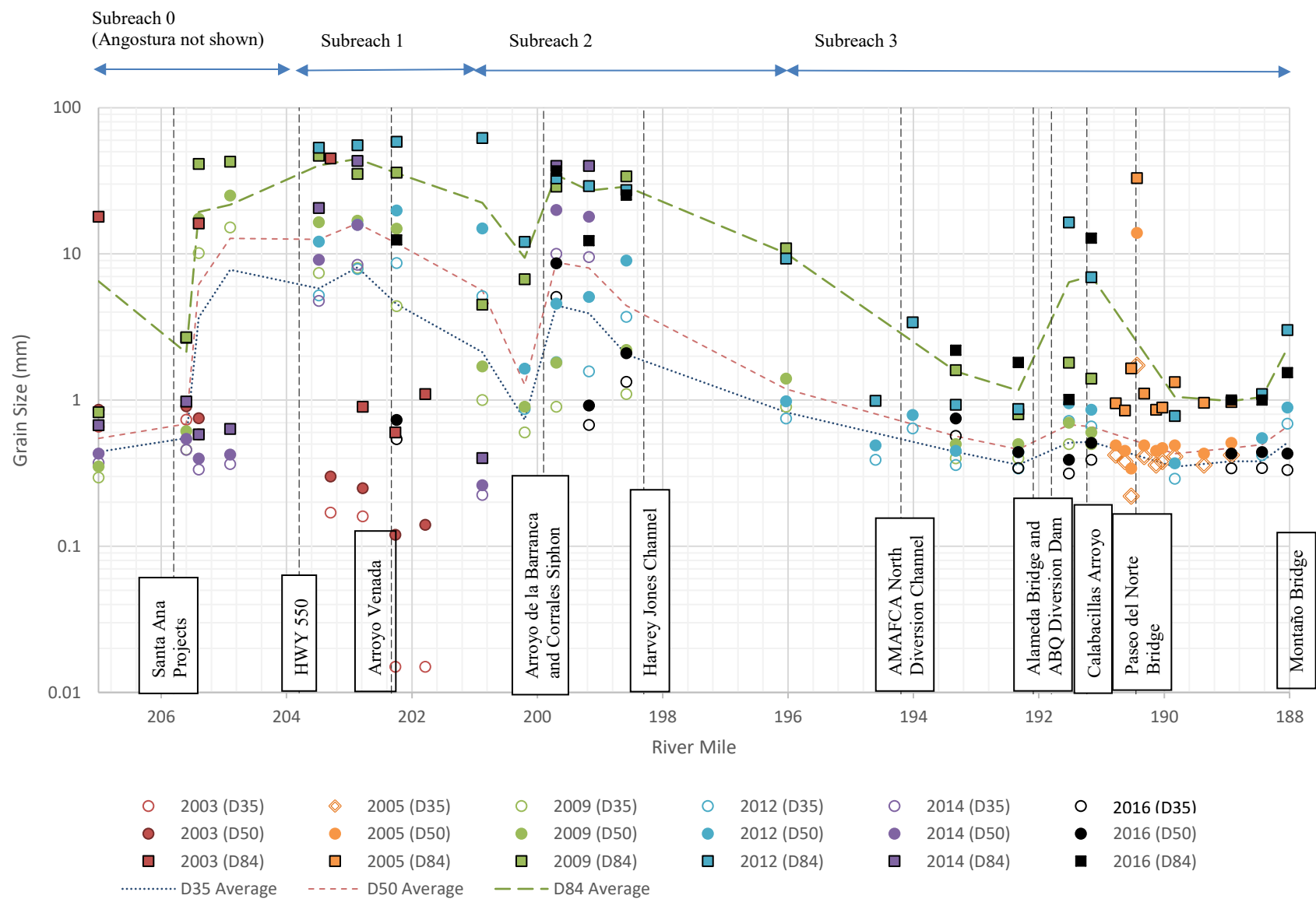


Figure 23 Recent bed material collection by grain size, year, and location.

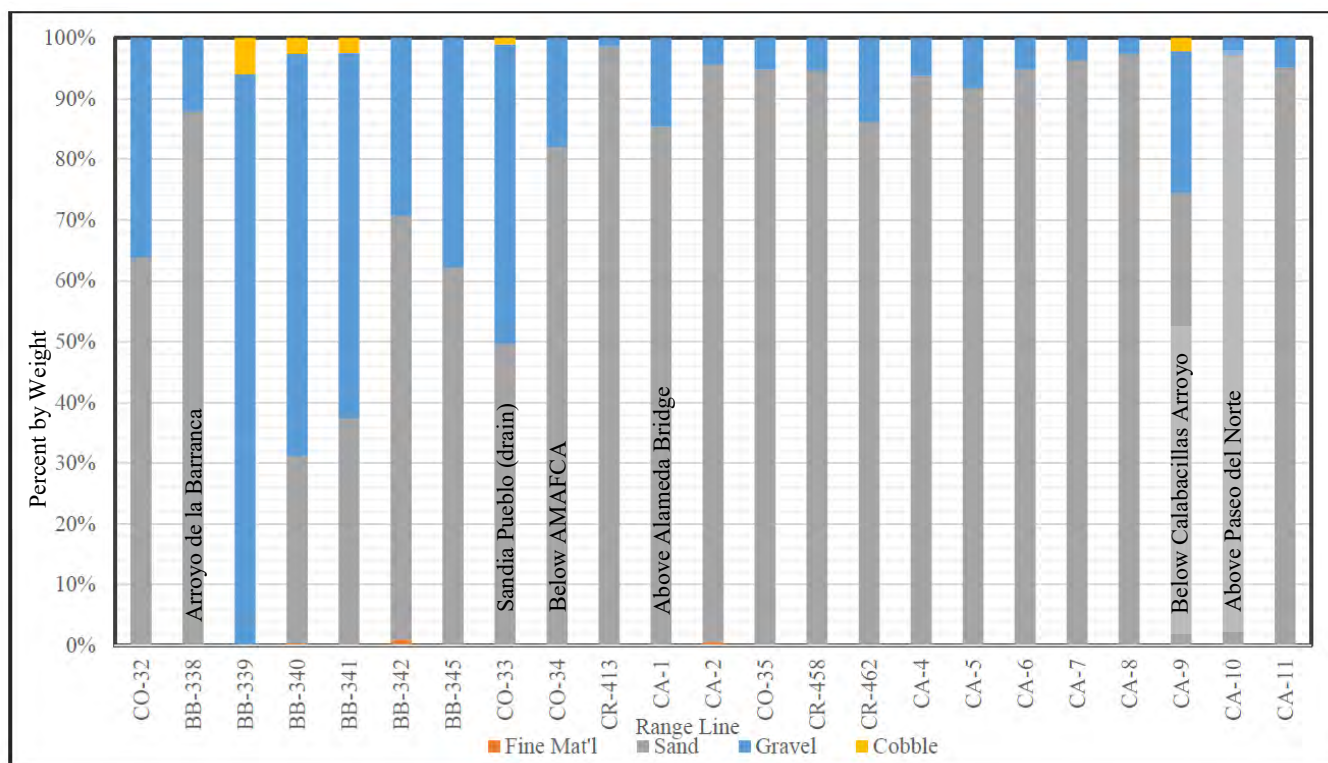


Figure 24 Percent bed material grain sizes for samples collected in February and March 2016 (modified from Tetra Tech, 2016).

3.6.2 Suspended sediment

Suspended sediment concentration has been shown to generally decrease with watershed urbanization and the installation of upstream dams and reservoirs. Table 12 shows a significant decrease in the suspended sediment concentration at the Albuquerque gage after the closure of Cochiti Dam. There was an increase of sediment concentration around 1990 (although the cause is unknown) (Makar and AuBuchon 2012).

Table 12 Average suspended sediment concentration of the Rio Grande at Albuquerque gage (USGS 08330000). Modified from Makar and AuBuchon 2012.

	1955-1975	1976-1990	1991-2005	2006-2014
Average concentration (mg/L)	3,377	499	831	760

For the period of record for the Albuquerque gage from 1970 to current, the annual tonnage of suspended sediment and the volume of water passing was calculated based on daily averages for suspended sediment (tons/day) and discharge (cubic feet per second). The two were plotted against each other in Figure 25. It becomes apparent in the trends that before the closure of Cochiti in the 1970s, there are significant peaks of suspended sediment discharged analogous to peaks of water conveyance. Since that time, the magnitude of sediment moved is much less in comparison to the water discharge. The more recent demonstration that suspended sediment does not increase in high water years indicates that sediment is limited from transport upstream of the reach. This is known as a supply limited reach.

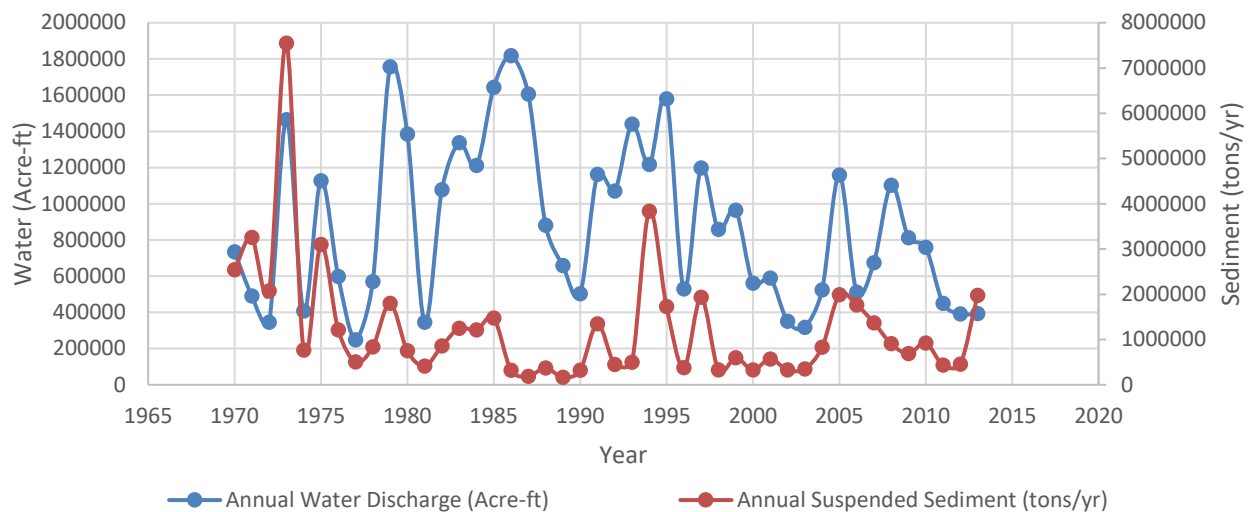


Figure 25 Annual totals for suspended sediment loads and the water discharge from the USGS gage at Albuquerque (USGS 08330000) from 1970 to 2013.

Statistical analysis was conducted to determine monthly patterns in suspended sediment transport and water conveyance (Figure 26). Generally, concurring with observations of Figure 27, the suspended sediment concentration is relatively consistent throughout the year, indicating that the sediment source of the reach is controlled or mitigated upstream. Water discharge is highest during the runoff from April to June, while the higher suspended sediment concentrations occur during post-runoff season, coinciding with monsoonal events from July to September.

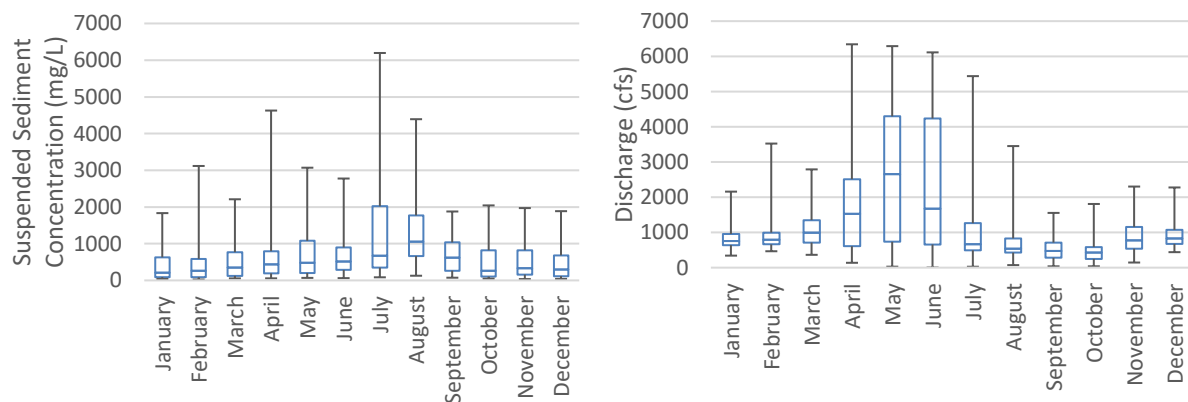


Figure 26 Monthly average box and whisker plots from 1970 to 2014 for the Albuquerque USGS gage. Whiskers indicate maximum and minimum, centerline in the box indicates median and surrounding quartiles representing the 25% and 75% values.

An effective discharge curve demonstrates the amount of sediment being moved at a particular discharge, and its peak indicates the hydrologic situation where the most work is done on the alluvial boundary. Biedenharn and Copeland's (2000) method was applied. The USGS field measurements of suspended sediment load at Albuquerque gage were used in this reach analysis. The field sediment discharge measurements were acquired daily during this time period. Flow duration curves by Bui (2014) were used to complete the analysis. Bui (2014) had separated the year into four hydrologic seasons that reflect the life stages for the Rio Grande silvery minnow.

For the sake of this study, pre-runoff and runoff season were combined to create three hydrologic seasons of equal duration: runoff (March through June), post-runoff or monsoon season (July through October) and winter (November through February).

The suspended sediment field-measured discharge was averaged for each water discharge interval, for each hydrologic season. A suspended sediment discharge rating curve was created to estimate the sediment discharge per water discharge interval, which was then multiplied by the annual frequency of these events, according to the Bui (2014) flow duration frequency.

The results (Figure 27) indicate that for the post-runoff or monsoon season 1,000 cfs is the most effective at transporting sediment in this reach. For the winter season approximately 1,100 cfs is the most effective in transporting sediment, and for the spring runoff season about 5,100 cfs is the most effective for transporting sediment. The fact that the post-runoff season has the highest sediment load in tons indicates the influence of upstream tributaries to the reach such as Jemez or other tributaries conveying sediment, some unchecked by upstream dams. The winter season is the least effective at transporting sediment.

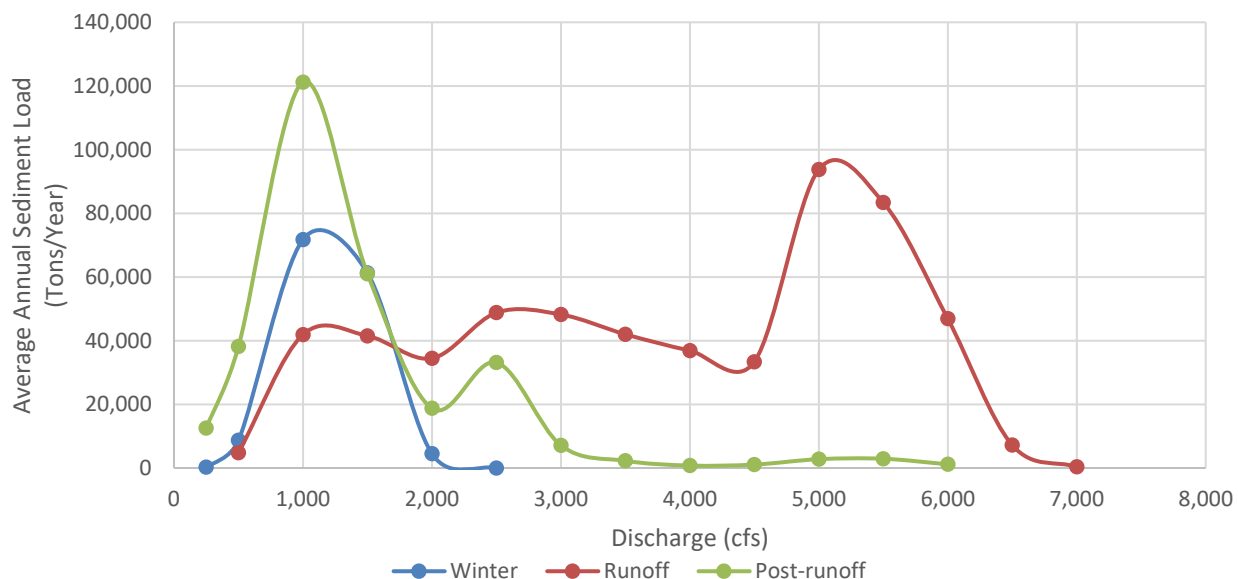


Figure 27 Effective discharge calculations demonstrating the hydrologic seasons and the sediment transported per unit discharge.

3.6.3 Total load calculations

During spring runoff in 2016, total load measurements were taken on five different dates at two cross sections within the Angostura Dam to Montañño Bridge Reach (Occam, 2016). The two locations of the total load data measurements during the 2016 spring runoff were at BB-309.5 and AQ-472.4. These locations represent the upstream and downstream ends of the study reach and are indicators for sediment inflow and outflow of the reach. The two cross sections were selected as they were at two relatively straight sections with a relatively uniform channel width. A straight section of a reach is preferred in sediment data collection as it reduces the likelihood of abrupt changes in velocity that could significantly alter the sediment load that is not representative of the reach. BB-309.5 is 1.2 miles downstream of HWY 550 Bridge, and AQ-272.4 is 0.8 mile downstream of the Montañño Bridge. BB-309.5, a temporary rangeline within

Subreach 1, is in a location of the reach where the bed material size was mostly categorized as gravel during the 2016 spring runoff (Table 13), while at AQ-472.4, the downstream temporary rangeline located below Subreach 3, is a location of the reach where the bed material would be categorized as sand during the 2016 spring runoff. These observations concur with trends in bed material identified in Section 3.6.1.

Figure 28 was created from twenty-two bed material samples collected at BB-309.5 (Upstream Section) and twenty-five bed material samples collected at AQ-472.4 (Downstream Section), collected in five different places across each rangeline on five different dates during spring runoff.

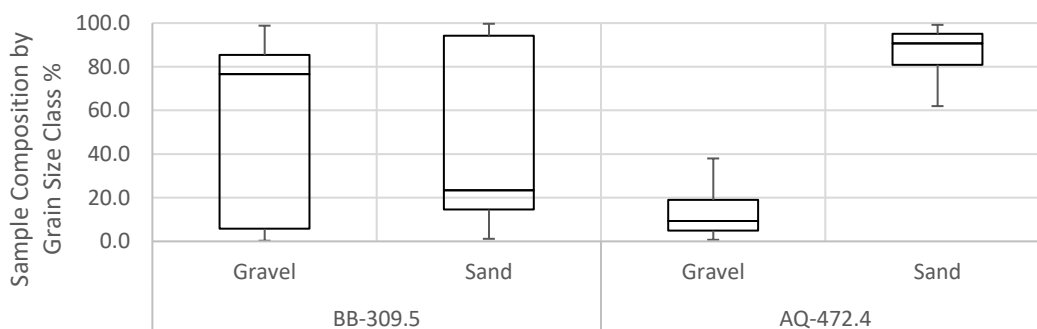


Figure 28 Box and whisker (error bars showing maximum and minimum values; Q1 (25%), median and Q3 (75%) represented by box bounds) averaging the results from sample collection during 2016 Spring Runoff (modified from Occam 2016).

Table 13 Sample results for Bed Material Sizes during 2016 Spring Runoff (modified from Occam 2016)

BB-309.5 Grain Size Distribution (mm)					
	Min	Q1 (25%)	Median	Q3 (75%)	Max
D84	0.36	0.87	28.82	33.60	65.96
D50	0.24	0.41	11.16	13.47	34.31
D16	0.17	0.30	0.55	1.51	16.06

AQ-472.4 Grain Size Distribution (mm)					
	Min	Q1 (25%)	Median	Q3 (75%)	Max
D84	0.36	0.59	1.01	1.40	2.73
D50	0.23	0.36	0.45	0.56	0.88
D16	0.15	0.20	0.22	0.26	0.38

The utilized method of total load data collection is equal discharge interval (EDI) with equal volume of suspended sediment and bed materials loads (Gray 2015). For both BB-309.5 and AQ-472.4, each cross section was divided into five columns of water where the discharges were measured to be relatively equivalent. The intention of the EDI with equal volume method was that each suspended sediment load measurement per water column has equal “weight” and can be composited into one suspended sediment load that represents a river cross section. The EDI with equal volume method was applied to bed materials at five locations per cross-section, so

that individual bed materials can be composited into one bed load measurement for the cross section. The combination of the composite suspended load and bed material load for the each cross-section at five different discharges on the rising and falling limbs of the 2016 spring runoff is the representative total load transported at the cross section.

The suspended and bed materials hydrographic measurements at BB-309.5 and AQ-472.4 were intended to be used in calculating the total sediment discharge with a software program called BORAMEP (Bureau of Reclamation Automated Modified Einstein Procedure). The total load discharge is intended to provide an estimate of the inflow and outflow of sediment to the reach at times during the rising and falling limbs of the spring snowmelt runoff season. In addition the measurements can be utilized to develop a rating function of sediment discharge vs. flow discharge.

Unfortunately, due to “insufficient overlapping bins” of grain sizes of bed material and suspended sediment at BB-309.5 and AQ-472.4, BORAMEP program could only produce two out of ten total load computations from the five days of data collection, and the two results were for AQ-472.4. Insufficient overlapping bins was found for the other AQ-472.4 samples and for BB-309.5 because the bed material consisted of mostly gravels, while the suspended sediment was predominantly fines and sands. This type of sediment distribution would be consistent with an armored bed condition. Without total load computations from BORAMEP at the incoming end of the reach, an overall picture of the incoming versus outgoing total loads could not be provided by this procedure.

An alternative computation for the total load is to use a bedload transport equation and combine the results with the suspended sediment load calculated from field measurements. Two empirical bedload transport equations based on excess shear stress were selected: The Surface-Based Bed Load Equation of Parker (1990) and the Surface-Based Relation of Wilcock and Crowe (2003). These were selected based on the available input data and the applicability of the equations. Wilcock and Crowe (2003) was developed for a full grain size distribution of the bed surface, including the sand, and includes an function that accounts for the nonlinear effect of sand content on gravel transport rates (Pitlick et al 2009). Parker (1990) was developed from a gravel-bed channel (Parker et al 1990) and thus is more applicable for the gravel-dominant BB-309.5 than for AQ-472.3, which is mostly sand (see Figure 28).

The required input variables for the computation of bedload using Parker (1990) and Wilcock and Crowe (2003) are

- Channel cross section stationing and elevation;
- Reach average water surface slope;
- Discharge;
- Bed surface grain size distribution.

Once the bedload values were obtained from the Parker equation and the Wilcock and Crowe equation, the suspended sediment load values from the 2016 measurements were added to obtain total load values. The suspended sediment load was calculated from the suspended sediment samples taken at each of the five EDIs and from the flow rate calculated for each EDI. The calculation took the weight of the dry sediment sample per volume of sample (mg/L) and

multiplied it by the EDI flow rate (ft^3/s). With the appropriate unit conversions, this provides a suspended sediment flow rate for the EDI in tons/day. All five EDIs were then added to obtain the suspended sediment load across the entire channel in tons/day.

Additionally, Yang's theoretical total load bed material transport capacity equation was conducted. This equation calculates the transport capacity of a river based on the available stream power. Yang's equation has the capability to perform total load computations for a sand bed as well as a gravel bed river system (Yang 1996). This approach is appropriate for both BB-309.5 and AQ-472.3, as these locations were respectively characterized as gravel and sand during the 2016 spring runoff (Table 13). Yang's original equation in 1972 for total load transport of sand bed materials emphasized the stream power available per a unit weight of water to transport sediments. He later calibrated the original equation for sand bed materials to develop the coefficients for an additional equation for gravel bed materials in 1984 (Yang 1996).

The required parameters for the computations of total loads at BB-309.5 and AQ-472.3 following Yang's equations are:

- Median particle size d_{50} : median size of bed materials within a water column of the cross sections;
- Velocity: the velocity of each of the five water columns at the two cross sections;
- Slope: slope of the bed near the two cross sections;
- Hydraulic depth: the hydraulic depth of each of the five water columns at the two cross sections;
- Channel width: the width of each of the five water columns at the two cross sections.

The total load values from each of these methods were plotted on **Error! Reference source not found.** along with the river discharge values for each measurement date. The total load values at BB-309.5 (just downstream of HWY 550) represent the incoming load, while the values at AQ-472.3 (just downstream of Montaña Bridge) represent the outgoing load. Table 14 provides the values for the suspended sediment load, bed load, and total load values for each of the equations on each of the measurement dates.

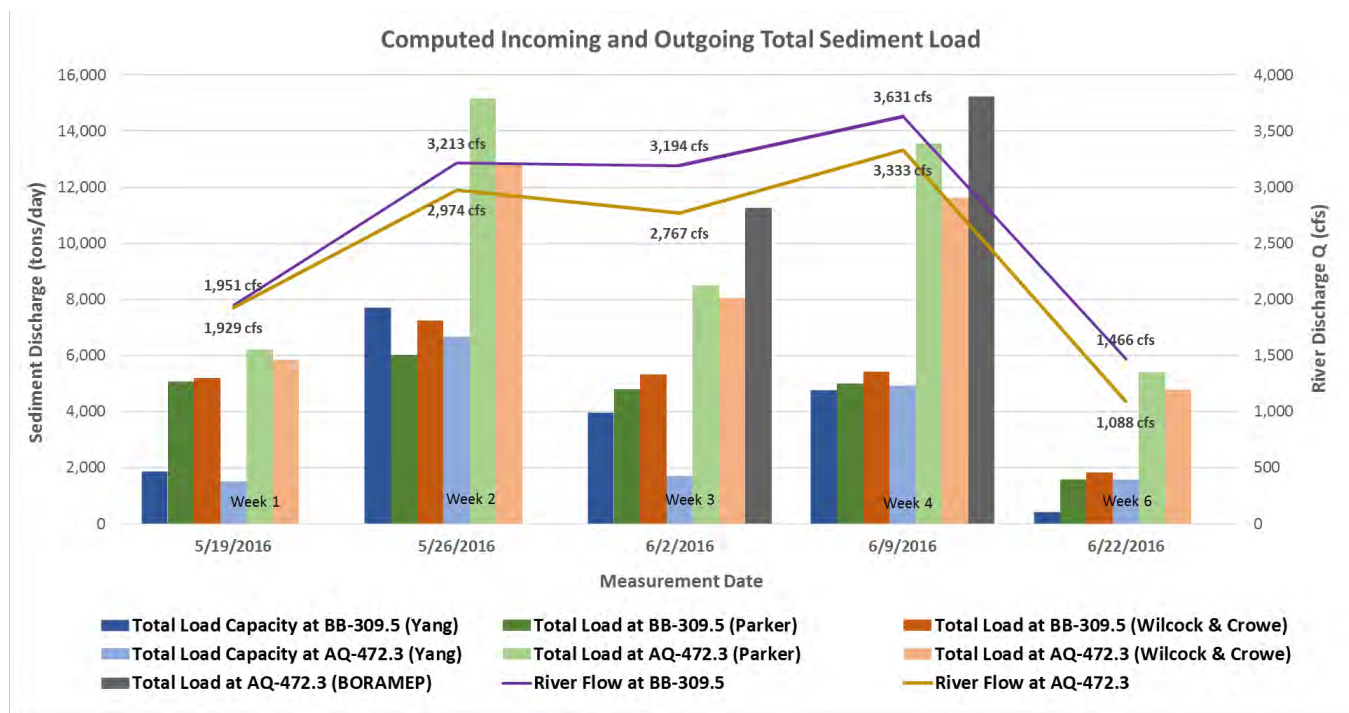


Figure 29 Computed Total Loads at the Incoming and Outgoing Cross Sections of the Reach between HWY 550 Bridge and Montañó Bridge

The calculated total load values do not vary proportionally with discharges. The computed total loads from May 26 have the highest values at the two cross sections, though this date does not correspond to the 2016 spring runoff peak discharge. The total loads increased while water discharges rapidly increased on the rising limb of the spring runoff. There was enough sediment stored in the reach after prolonged periods of low flows that was mobilized as flows increased from the first to the second week of the 2016 spring runoff. The discharges of the third week of the 2016 spring runoff (June 2) slightly decreased from the discharges of the second week, but the computed total loads decrease significantly. The decrease in the total loads might have been due to the stored sediments on the bed being mostly mobilized, leaving the stream with excess sediment transport capacity. The computed total loads of the fourth week pick up with increasing flows to the peak discharges of the 2016 spring runoff. The increase in the total loads might have been due to excess stream power that started eroding banklines. It was noticed during the 2016 spring runoff that the west bankline immediately downstream of HWY 550, the east and west banklines at Sandia Priority Site, and the east and west banklines downstream of Corrales Siphon experienced active bankline erosion. As flows tapered down on the falling limb of the 2016 spring runoff hydrograph, the computed total loads also rapidly decreased.

When examining the incoming load versus the outgoing load for each equation, it is noticed that the results from the Parker equation and the Wilcock and Crowe equation have a higher outgoing load than incoming load for each measurement date. This suggests that the river is gaining sediment from the bed (incision), banks (erosion), and/or tributary inputs.

Table 14 Computed Total Loads at the Incoming and Outgoing Cross Sections of the Reach between HWY 550 Bridge and Montañño Bridge

Equation	BB-309.5 (Upstream)					AQ-472.3 (Downstream)				
	Date	Discharge (cfs)	Suspended Load (tons/day)	Bed Load (tons/day)	Total Load (tons/day)	Date	Discharge (cfs)	Suspended Load (tons/day)	Bed Load (tons/day)	Total Load (tons/day)
Yang	5/19/2016	1,951	N/A		1,861	5/20/2016	1,929	N/A		1,506
Parker			5,056	20	5,076			5,013	1,216	6,229
Wilcock and Crowe				150	5,206				830	5,843
Yang	5/26/2016	3,213	N/A		7,702	5/27/2016	2,974	N/A		6,663
Parker			5,607	418	6,025			9,236	5,935	15,171
Wilcock and Crowe				1,643	7,249				3,607	12,844
Yang	6/2/2016	3,194	N/A		3,951	6/3/2016	2,767	N/A		1,715
Parker			4,784	6	4,790			7,030	1,465	8,496
Wilcock and Crowe				534	5,318				1,023	8,054
BORAMEP				N/A	N/A				4,238	11,268
Yang	6/9/2016	3,631	N/A		4,771	6/10/2016	3,333	N/A		4,913
Parker			4,984	4	4,988			8,484	5,077	13,561
Wilcock and Crowe				431	5,414				3,134	11,619
BORAMEP				N/A	N/A				6,746	15,231
Yang	6/22/2016	1,466	N/A		409	6/23/2016	1,088	N/A		1,567
Parker			1,566	2	1,568			3,762	1,637	5,399
Wilcock and Crowe				259	1,824				1,002	4,764

However, the Yang equation has a lower outgoing load than the incoming load for the first three measurement dates, but reversed for the last two measurement dates. This suggests that the reach is depositing sediment out of the river flow onto the bed and/or banks (aggradation) for the first three weeks, but losing sediment between weeks four and six. A rough analysis of the difference between the incoming and outgoing load cumulated over the six weeks suggests an overall aggrading trend for the Yang equation load values.

To compare these observations with actual bed elevation observations, the longitudinal profile (Figure 30) is revisited from Section 3.1. The longitudinal profile shows that the river bed elevation between HWY 550 to just downstream of Harvey Jones Channel (RM-196.6) has incised 2-3 feet between 2009 and 2017. Downstream of RM-196.6, the river bed has remained at approximately the same elevation, even increasing in bed elevation between 2009 and 2017. Thus, considering the spatially and temporally varying bed trends, the total load results discussed above cannot be singularly applied to the actual observations of the longitudinal profile, likely because the total load calculations being based on a single event with non-continuous measurements.

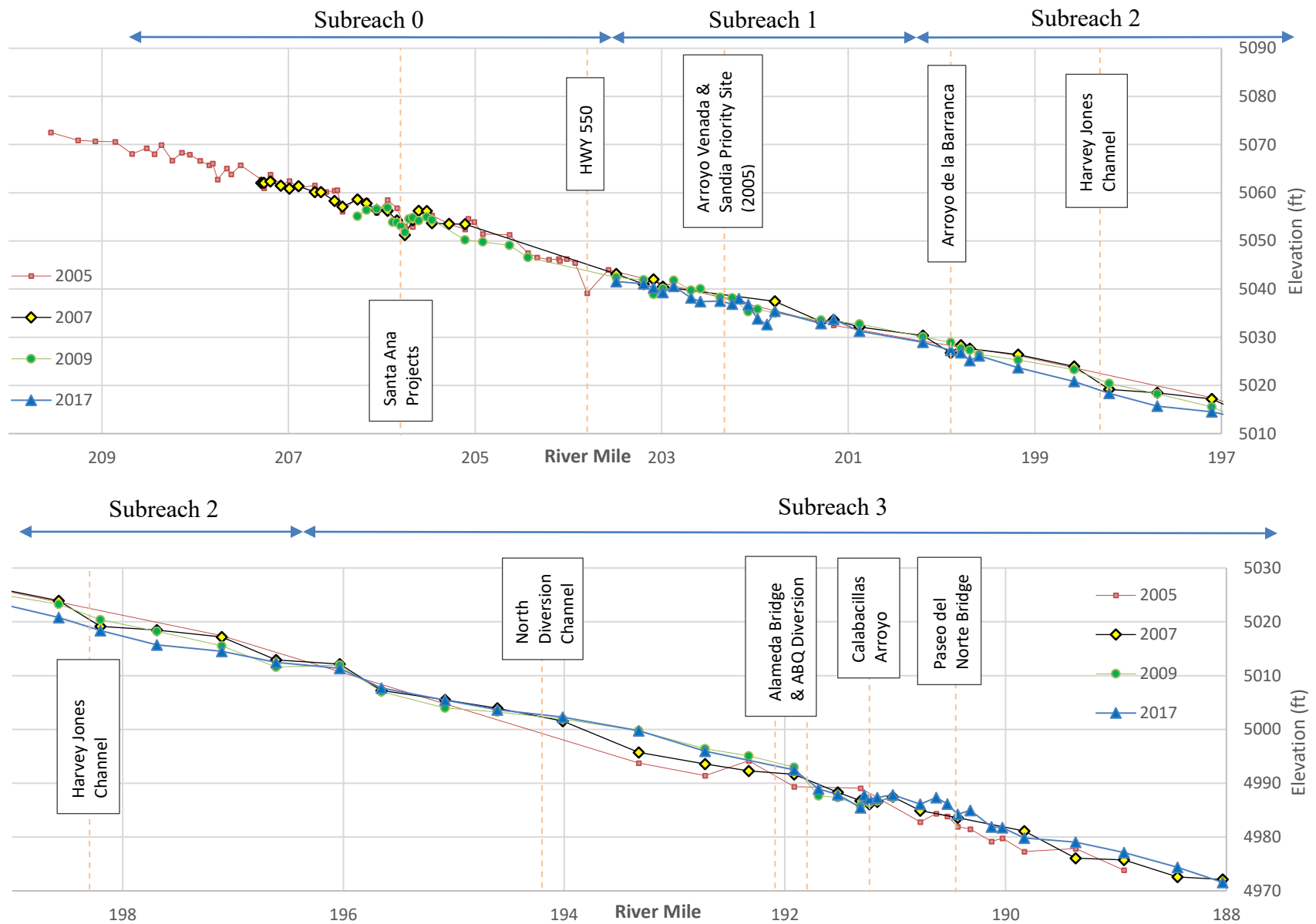


Figure 30 Channel Bed Elevation of the Study Reach in recent years

3.6.4 SRH-1D Technical Report Summary

The Bureau of Reclamation Technical Service Center (TSC) developed a one-dimensional sediment transport model to predict future channel response to different hydrologic regimes. The model covers the Middle Rio Grande from Angostura Diversion Dam to Isleta Diversion Dam. The model development, calibration, and results are documented in the 2018 Technical Report titled "SRH-1D Numerical Model for the Middle Rio Grande Angostura Diversion Dam to Isleta Diversion Dam" (Varyu 2018). The report is summarized here.

The sediment model was calibrated based on predicted changes in channel sediment storage as compared to the observed data. The calibration used historical data from 2002 to 2012 as its observed data. The calibrated model was used to predict future sedimentation trends for a twenty year period for three hydrologic regimes: wet, average, and dry.

The model calibration results are summarized as:

- The numerical model reproduced the general shape and magnitude of the cumulative erosion and deposition in the main channel from 2002 through 2012.
- Net volume loss (erosion and/or channel widening) was observed from Angostura Diversion Dam to about the Harvey Jones Channel. Net volume gain (bed aggradation or channel narrowing) was observed from the Harvey Jones Channel to Isleta Diversion Dam.
- The total cumulative observed deposition in the main channel of about 1000 acre-ft was simulated by the calibration run to be 910 ac-ft, with observed maximum cumulative erosion near the Harvey Jones Channel of about 500 acre-ft being simulated at 600 ac-ft.
- The floodplain remained stable (experiencing neither aggradation nor degradation) during the calibration period.
- Parker sediment transport equation (with a non-dimensional reference shear stress of 0.035 and a hiding factor of 0.67) predicted the best results in this gravel/sand reach. The numerical model was most sensitive to the sediment transport equation used, and the minimization parameter 'wfrac'. Model results are effected to a lesser degree to active layer thickness, upstream sediment supply, and Manning roughness coefficient.

The calibrated model is used to predict future river response in 20 years with dry, average, and wet hydrologic regimes. Predictions of future trends are summarized as:

- Continued net loss of channel volume is likely upstream of the ABCWUA diversion.
- Continued net accumulation of sediment volume is likely downstream of the ABCWUA diversion.
- A total about 1000 acre-ft of sediment will be removed in the 40 mile study reach from Angostura Diversion Dam to Isleta Diversion Dam, with the dry hydrologic regime halving the amount of net channel loss and the wet hydrology doubling it.
- Predicted changes in sediment size are insensitive to future hydrology in the study reach.
- Some potential implications of this predictive modeling could include the following:
 - Locations of channel bed lowering (upstream of ABCWUA diversion) could lead to bank erosion, a loss of floodplain connectivity, and a loss of endangered species habitat

- Locations of aggradation (sediment volume accumulation) could cause reduced channel capacity and increase floodplain connectivity and potential habitat.

4.0 Hydrologic Analysis

Before flood control and water supply operations, the annual peak flows varied greatly. As shown in Figure 31, the discharges exceeding 5000 cfs were more frequent before water operations began in the 1970s. There were also frequently years where the discharge exceeding 500 cfs throughout the year occurred fewer than 150 days for the year. The episodes of dry and wet periods were sporadic. Water operations has decreased the variability in discharge, causing the Middle Rio Grande to be wet for a greater period of the year, but at lower peak discharges than previously observed. Discharge events exceeding 5000 cfs in the current, regulated system, are rare.

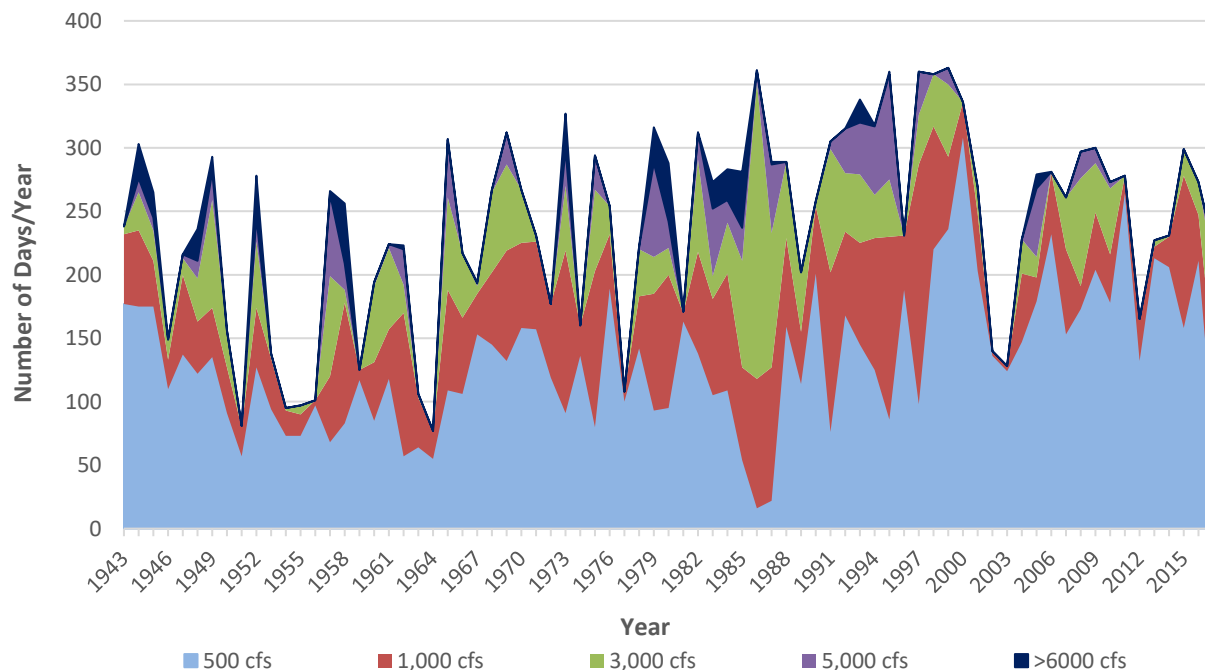


Figure 31 Number of days each year exceeding set discharges for the USGS gage on the Rio Grande at Albuquerque for period of record (USGS 08330000).

Bui conducted analysis of discharges according to seasonal periods that are hydrologically relevant (2014): Pre- and post-runoff, runoff and winter flows from 1993 to 2013 (Figure 32). The pre-runoff constituted discharges from March to April; runoff from May to June; post-runoff or monsoon season from July to October; and winter from November to February. For the Albuquerque gage (USGS 08330000), it was shown that during the winter flows, discharges rarely exceed 1,000 cfs. Discharge events exceeding 5,000 cfs account for less than 1% of the daily average discharges found in the Middle Rio Grande in this reach for the year. As shown in Figure 32, the runoff season has the highest probability of exceeding a given discharge.

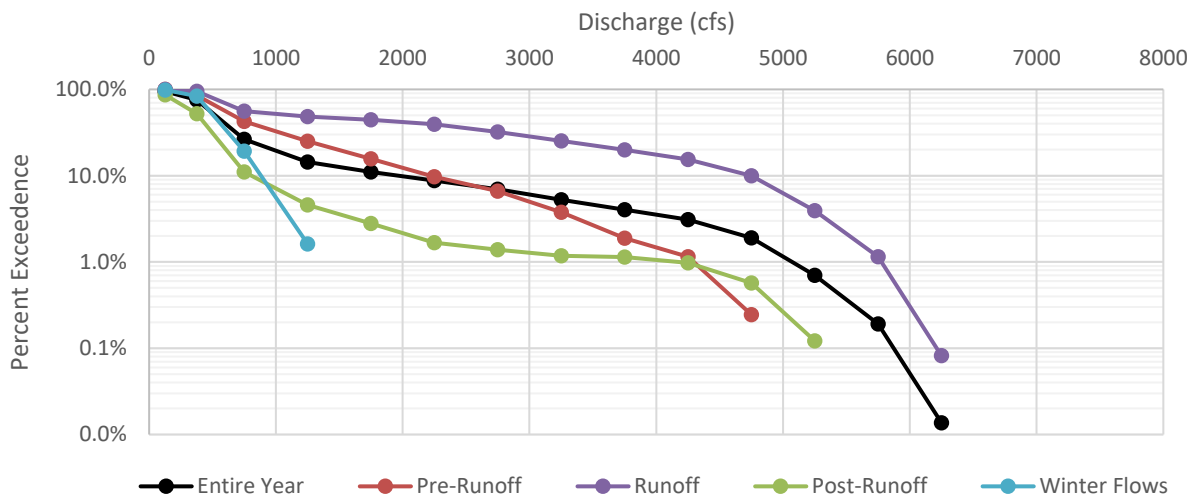


Figure 32 Percent exceedance for particular discharge intervals from 1993 to 2013. Modified from Bui 2014.

4.1 Floodplain Terraces

Terraces are swaths of flat or gently sloped areas of varying heights in comparison to the baseflow of a river. They are often generated from abandoned river flood plains, as the river changes its course through time due to deposition, or they are generated as the river incises and drops below its former floodplain. Reconnecting terraces is an opportunity for habitat enhancement. High terraces may be undermined and easily eroded because the erosive forces occur below the root line of the bank vegetation. This phenomenon was observed by Massong at Arroyo de las Cañas Priority Site (2006).

Using 2012 LiDAR imagery, the river water surface elevation along the Rio Grande active channel was extracted. LiDAR does not allow for capture of bathymetric surfaces, and instead captures the elevation of the water surface. The 2012 LiDAR was collected at a discharge of about 800 cfs, so flow would have been within the active banks of the Rio Grande throughout this reach. The water surface elevation of the 2012 LiDAR was extracted into a raster, then converted to a polygon so that the water surface elevation of the the 800-cfs condition can be generated beyond extents of the river banks to the surrounding terrain. It should be noted that this operation required the water surface raster to be rounded to integer values. Therefore, the accuracy of the water surface shown in Figure 30 is within 1 ft. Once a buffer was applied to extend the raster beyond the river surface, the polygon was converted to a raster again so that spatial analysis could be conducted. The water surface elevation was subtracted from the surrounding terrain elevations. The result is a raster showing terraces and their elevation above (i.e. relative to) the 800-cfs water surface elevation (datum).

To optimize habitat restoration opportunities for the Rio Grande silvery minnow, the ideal design would be inundated for at least 14 days during the peak runoff (Bachus and Gonzales, 2017), as this 14-day period is thought to be the minimum time supportive of initial development of newly hatched Rio Grande silvery minnow. The daily reported discharge graphs for the Albuquerque USGS gage 08330000 were analyzed for March 1 through July 1 for every year from 1993 to 2016, which was identified as the drier hydrologic cycle on the Middle Rio Grande that is more

representative of the current hydrologic regime (Holste 2013). The peak was defined as 14 consecutive days with the highest persistent discharge for the time period. The minimum discharge of this 14-day event was recorded. Pearson Type III analysis was conducted on the log transform, fitting the distribution to a 2-year frequency curve (Belmont, 2015). For the Albuquerque USGS gage 08330000, it was found that the 14-day spring runoff flow magnitude with 50% chance of exceedance is 1870 cfs.

The HEC-RAS model representing 2012 rangeline geometry was run at 800 cfs and 1800 cfs to represent the estimated water surface for the 2012 LiDAR and the 14-day spring runoff flow magnitude with 50% chance of exceedance respectively. The water surface elevation (WSE) for both simulations was extracted from the model results, and subtracted from one another. The difference of WSE for the two HEC-RAS simulations for each cross section was averaged to determine a reasonable WSE to expect inundation from the spatial, floodplain terrace analysis in ArcGIS. The average WSE difference between 800 cfs and 1800 cfs was found to be 1.44 feet, with maximums at around 1.93 feet in the Angostura to HWY 550 portion of the reach, to a difference of 0.6 feet progressing downstream.

The symbology of the flood plain terrace map was adjusted to better demonstrate important considerations for potential river maintenance and habitat restoration alternatives:

Legend Color (Figures 32 A-E)	Descriptor in Legend	Terrace Analysis Results - Height above LiDAR WSE (800 cfs)
Light Blue	Below WSE/WSE	Less than 0 ft
Yellow	WSE; Inundation in Subreach 3	0 ft – 0.75 ft
Blue	Inundation likely at slightly less than 2-year frequency; less likely in Subreach 0 (1800 cfs)	0.75 ft – 1.5 ft
Green	Begin Minimal Excavation (for Inundation Design Discharge - 1800 cfs)	1.5 ft – 3.0 ft
Orange	Begin Moderate (Restrictive) Amount of Excavation	3.0 ft- 5 ft
Black	Begin Significant (Prohibitive) Amount of Excavation	5 ft – 7 ft
White	Exceeds 7 ft above WSE; not realistic for project design requiring excavation	More than 7 ft

Generally, it was found that the surrounding floodplain is higher than the river location. This conforms to the historical observations that the river was historically aggrading and is now incising. It was found that the top of the reach, between Angostura Diversion Dam and BB-340, is constrained by higher terraces (Figure 33A and B). At HWY 550, there are lower terraces near the river banks to the river's west side, though these exceed the water surface by over 5 feet (Figure 33B). From BB-345 to the Alameda Bridge near CA-4, the elevation of the surrounding floodplain is of a lower elevation surrounding both sides of the river channel relative to the

A) Angostura Dam to CO-29

River direction

0 0.25 0.5 1 mile

Legend

Floodplain Terraces

- Below WSE/WSE
- WSE
- Likely Inundation (1800 cfs)
- Minimal Excavation for Inundation
- Restrictive Amount of Excavation
- Prohibitive Amount of Excavation
- Exceeds 7 ft above WSE

Source: Esri, DigitalGlobe, GeoEye, Earthstar Geographics, CNES/Airbus DS, USDA, AeroGRID, IGN, etc.

B) BI-286 to HWY 550 to BB-342

River direction

HWY 550

BB-342

Legend

Floodplain Terraces

- Below WSE/WSE
- WSE
- Likely Inundation (1800 cfs)
- Minimal Excavation for Inundation
- Restrictive Amount of Excavation
- Prohibitive Amount of Excavation
- Exceeds 7 ft above WSE

0 0.25 0.5 1 Miles

1 mile

Source: Bay Conservation & Development Act, San Francisco Bay, California, 1972

C) BB-342
to CR-372

River direction

Legend

Floodplain Terraces

- Below WSE/WSE
- WSE
- Likely Inundation (1800 cfs)
- Minimal Excavation for Inundation
- Restrictive Amount of Excavation
- Prohibitive Amount of Excavation
- Exceeds 7 ft above WSE

0 0.25 0.5 1 Miles

1 mile

Source: Esri, DigitalGlobe, GeoEye, Earthstar Geographics, CNES/Airbus DS, USDA, AeroGRID, IGN, SRTM3, and the GEBCO Project

D) CR-378 to through AMAFCA North
Diversion Channel to through Alameda Bridge

Legend

Floodplain Terraces

- Below WSE/WSE
- WSE
- Likely Inundation (1800 cfs)
- Minimal Excavation for Inundation
- Restrictive Amount of Excavation
- Prohibitive Amount of Excavation
- Exceeds 7 ft above WSE

0 1 mile

E) CA-3 through Paseo del Norte Bridge through Montañño Bridge to AQ-467

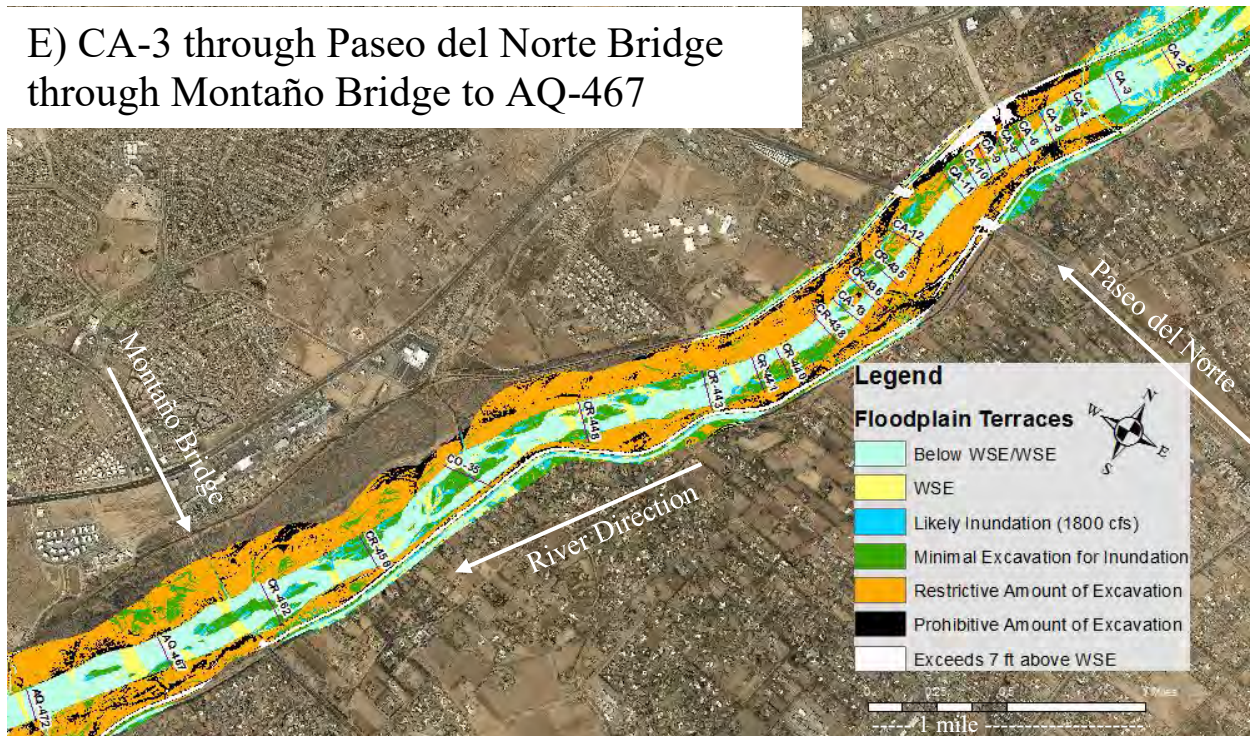


Figure 33 Terrace analysis results for the study reach. Figures A-E progress downstream through the reach.

5.0 Future Channel Response

As identified from the various hydrographic trends throughout the report, the expected trends generally conform to Schumm's (1977) and Massong's et al. (2010) models. Each of these topics have been covered more in depth throughout the report, but a summary follows.

As the peak discharge decreases, so will the channel width. As vegetation encroaches on the narrowing channel and on sand bars, average channel depth will increase, indicating incision. The incised channel will support increased bend migration, as the incised conditions and more concentrated flows will undermine the roots of surrounding vegetation. Given this process the encroaching vegetation may not necessarily stabilize the banks in place. The lateral migration will also be exacerbated by the trends of river bed coarsening, as the sediment starved reach will uptake sediment from the river banks if the bed material is too coarse. The reach will experience decreasing slope as sinuosity increases. The sinuosity (channel length: valley length) is affected by changes in belt width and meander wavelengths, which affects the river length. Deposition was identified near the AMAFCA channel in the lower part of the reach study. The lower reach has a finer bed material than the rest of the reach.

Problems arising from these trends were identified as bend migration affecting infrastructure, as well as infrastructure confining the migration of the channel to naturally progress to cutoff channels (M7) as described by Massong's et al. (2010) planform model. The lateral migration and bank erosion may lead to the loss of terrestrial habitat and future river maintenance issues. The disconnected floodplain due to channel incision is not the best

situation for maintenance of endangered species habitat. The planform stages and in-channel processes does allow for point bar formation and the development of new floodplain habitat in areas of deposition on the point bar surface. This process is the river's way of creating a new floodplain in the incising areas. Subreach 3, especially upstream of the San Juan Chama drinking water diversion, shows some areas of deposition; however, the lower parts of the reach study in Subreach 3 may have capacity issues in the future. The channel spanning surface diversion and its backwater created by the checking up of the water surface elevation acts as a both local bed slope and hydraulic river control. Projects to reconnect the floodplain may be more viable in this location, as the trend is an increasing bed elevation.

Potential engineering methods to address these trends are to reduce erosive trends by increasing the sediment supply in the reach, such as by reconnecting arroyos or investigating the sediment management practices throughout the reach. Mowing and destabilizing vegetated islands can support a mobilized sand bed channel and may also increase sediment supply. Mowing however may remove some valuable riparian habitat, and if flows are not significant, vegetation encroachment and stabilization may occur again. Increasing the floodplain buffer and allowing the meander bends to deepen allows floodplain habitat to develop on the inside of the bend (point bar surfaces). Designing cutoff/secondary channels or creating a floodplain in the active channel at its incised elevation may act to reset the channel planform and allow the channel to continue dynamic progression as it adjusts to starved sediment loads and reduced peak discharges.

6.0 Acknowledgements

A significant amount of this work was curated by Tetra Tech's HWY 550 to Montañito Geomorphic Assessment (2013), as well as data analysis conducted by the Bureau of Reclamation in the 2000s, and Mussetter Engineering, Inc.'s (MEI) analysis in 2002. Collaboration with Santa Ana Pueblo allowed for the study reach to extend upstream from HWY 550 to Angostura Diversion Dam near Jemez Canyon.

7.0 References

Bachus, J. and Gonzales, E. (2017) *Technical Note: Habitat Targets for BdA Realignment Pilot Modeling Analysis*. Albuquerque, NM.

Belmont, P. (2015) *Flood Frequency Analysis*. Utah Watershed Coordinators Workshop. Utah State University. Logan, UT.

Berry, K. and Lewis, K. (1997) *Historical Documentation of Middle Rio Grande Flood Protection Projects, Corrales to San Marcial*. Prepared for US Army Corps of Engineers, Albuquerque District. Office of Contract Archaeology, University of New Mexico. OCA/UNM Report No. 185-555. Albuquerque, NM.

Biedenharn, D. and Copeland, R. (2000) *Effective Discharge Calculation. Technical Note*, US Army Corps of Engineers. Vicksburg, MS.

Bui, C. (2017). *2017 Spring Runoff Monitoring Assessment*. Albuquerque, NM.

Bui, C. (2014). *Flow Duration Curve from Cochiti to Elephant Butte*. Albuquerque, NM.

Crawford, C., Cully, A., Leutheuser, R., Sifuentes, M., White, L., and Wilber, J. (1993). *Middle Rio Grande Ecosystem Bosque Biological Management Plan*. Middle Rio Grande Biological Interagency Team. Albuquerque, NM.

Gray, J. (2015). "Sediment Data Collection Training Course". USGS. Reston, VA.

Heo, J., Duc, T., Cho, H., Choi, S. (2009) *Characterization and prediction of meandering channel migration in the GIS environment: A case study of the Sabine River in the USA*. Environmental Monitoring Assessment. 152:155.

Holste, N. (2013). *Geomorphic Assessment of the Rio Grande Upstream of Elephant Butte Reservoir*. Albuquerque, New Mexico.

Klein, M., and Bui, C. (2016). *2016 Spring Runoff Weekly Monitoring Assessment*. Albuquerque, NM.

Makar, P. and AuBuchon, J. (2012). *Channel Conditions and Dynamics of the Middle Rio Grande River*. Lakewood, CO.

Massong, T., Makar, P., Bauer, T. (2010). *Planform Evolution Model for the Middle Rio Grande, New Mexico*. 2nd Joint Federal Interagency Conference, Las Vegas, NV.

Massong, T. (2006). *River Maintenance Priority Sites near Arroyo de las Cañas, Geomorphic Trends Assessment*. Albuquerque, NM.

Middle Rio Grande Conservancy District (MRGCD). (2014). *Draft Technical Memo Condition Assessment: Corrales Siphon Rio Grande crossing South of Arroyo de la Barranca*. Albuquerque, NM.

Mussetter Engineering, Inc (MEI). (2002). *Geomorphic and Sedimentologic Investigations of the Middle Rio Grande between Cochiti Dam and Elephant Butte Reservoir*. Fort Collins, Colorado

Nemeth, M. and Sixta, M. (2005). *Sandia Priority Site Project Description*, Albuquerque, NM.

New Mexico Interstate Stream Commission (NMISC). (2016). *Phase 2 – Rio Rancho Open Space Habitat Restoration Project; Project Summary and As-Built Report*. In collaboration with City of Rio Rancho Parks, Friends of Rio Rancho Open Space.

Occam/EC (2016). *2016 Total Load Measurement Report May and June of 2016*. In collaboration with Tetra Tech. Albuquerque, NM.

Parker, G. 1990. Surface-based bedload transport relation for gravel rivers. *Journal of Hydraulic Research*, Volume 28– Issue 4, pp 417-436.

Pitlick, John; Cui, Yantao; Wilcock, Peter 2009. Manual for computing bed load transport using BAGS (Bedload Assessment for Gravel-bed Streams) Software. Gen. Tech. Rep. RMRS-GTR-223. Fort Collins, CO: U.S. Department of Agriculture, Forest Service, Rocky Mountain Research Station. 45 p.

Reclamation (2017). *Geomorphic and Hydraulic Assessment of Sandia Pueblo Bendway Weir Repairs*. Albuquerque, NM.

Reclamation (2016). *As-Built Data Report Collection for the Corrales Siphon*. Albuquerque, NM.

Reclamation. (2007). *Middle Rio Grande River Maintenance Plant Part 1 Report*. Albuquerque, NM.

Richard, G. (2001). *Quantification and Prediction of Lateral Channel Adjustments Downstream from Cochiti Dam, Rio Grande, NM*. Fort Collins, CO.

Schumm, S. (1977). *The Fluvial System*. Blackburn Press. Ft Collins, CO.

Sixta, M. and Nemeth, M. (2005). *Bernalillo Priority Site Project Description*. Albuquerque, NM.

Tetra Tech. (2013). *Geomorphic and Hydraulic Assessment of the Rio Grande from US Highway 550 Bridge to Montañño Bridge - 2004 to 2012*. Albuquerque, NM.

Tetra Tech (2016). *Middle Rio Grande Project Hydrographic Data Collection; Field Data Collection Report; Cross-Section Surveys; Bernalillo to Montañño Lines Surveys*. February 2016. Albuquerque, NM.

Varyu, D. (2018). *SRH-1D Numerical Model for the Middle Rio Grande: Angostura Diversion Dam to Isleta Diversion Dam*. Denver, CO.

Wright, J. M., Dworak, F. J., and England Jr., J. F. (2010). *Middle Rio Grande Peak Discharge Frequency Study*. Denver, CO.

Yang, C. T. (1996). *Sediment Transport Theory and Practice*. McGraw-Hill Companies, Inc.